A Reproduced Copy

OF

NASA CR-166,421

Reproduced for NASA

by the

NASA Scientific and Technical Information Facility

FFNo 672 Aug 65

Analysis of a Finite Difference Grid

G. H. Klopfer

NASA

N93-13071

Analysis of a Finite Difference Grid

Goetz H. Klopfer
Nielsen Engineering & Research, Inc.
Mountain View, California

NASA

TABLE OF CONTENTS

ANALYSIS OF A FINITE DIFFERENCE GRID

Goetz H. Klopfer
Nielsen Engineering & Research, Inc.

SUMMARY

Some means of assessing the suitability of a mesh network for a finite difference calculation are investigated in this study. This has been done by a study of the nonlinear truncation errors of the scheme. It turns out that the mesh can not be properly assessed a priori. The effect of the mesh on the numerical solution depends on several factors including the mesh itself, the numerical algorithm, and the solution. Several recommendations are made with regard to generating the mesh and to assessing its suitability for a particular numerical calculation.

INTRODUCTION

One of the most important problems that arises in finite difference solutions to physical problems is the·quality of the grid used in the calculation. For simple configurations, e.g., two dimensional problems, a conformal transformation which gives an orthogonal grid can be used. This still leaves the questions of the adequacy of the grid clustering unanswered. In complex problems the grid may not be orthogonal, and a question of the effect of grid skewness on the solution accuracy arise. In addition to these problems of grid clustering and skewness, it is desirable to determine whether the grid is sufficiently fine to capture the detailed physics of the flow, especially if the location of phenomena like shock waves change during the solution. Other critiera (e.g., smoothness) may also be important.

At present the only way of determining the suitability of a grid is by visual examination, and while this may be satisfactory for simple geometries, it is an almost impossible

task for complex geometries. It would be extremely useful, therefore, to derive some criteria to measure the suitability of a grid that could be determined computationally. The quality of a complex three dimensional grid could thus be determined before a lengthy flow solution is attempted.

In a general two dimensional grid the coordinate transformation $\tau = t$, $\xi = \xi(t,x,y)$, $\eta = \eta(t,x,y)$ permits clustering and spreading of the points in two-dimensions. The components of the Jacobian transformation matrix (hereafter called "metrics") x_ξ, y_ξ and x_η, y_η can be examined to determine the quality of a grid. The main problem is to decide the attributes of a good grid; it is anticipated that quantities such as curvature variation, Jacobian variation, skewness and volume of grid cells, in addition to other geometric quantities will be important.

First the attributes of a good grid are determined, and second, means of quantifying the grid quality are developed. In addition to this purely geometric problem, it is likely that the relative quality of a grid will depend on the algorithm in the code since the major aim is to reduce the truncation error. Since different algorithms have different truncation errors it is probable that grid quality is dependent on the algorithm and the solution. A particular algorithm is chosen for more detailed study.

Finally, a feasibility analysis on the extension of the above criteria to three dimensions is undertaken.

COMMENTS ON MESH CRITERIA

Before some criteria can be established which will serve to quantify a "good" mesh, it is necessary to discuss the various purposes a mesh needs to serve. This will be done in this section. The discussion will be limited to problems applicable in computational fluid dynamics.

2

For an ideal incompressible flow, finding the solution is tantamount to finding the coordinate lines. This is of course the motivation of conformal mappings. The solution and the mesh are given in terms of level curves of potential and stream functions. Extensions of this idea to compressible flows has not been as successful. For example, the "contour dynamics" scheme of Harlow (Ref. 1) recast the problem as finding the locations of level curves of density, pressure, and velocities. While the problem of establishing the mesh is circumvented, other more severe and less tractable difficulties arose.

Another method of avoiding the mesh generation problem is by the use of Lagrangian variables (Ref. 2). In these variables the mesh node points move with the fluid velocity and thus the mesh is automatically generated. The unsolved problem with this approach is the excessive mesh distortion at stagnation points or in the viscous layer. This distortion causes accuracy and stability problems. Attempts have been made to solve this problem by remeshing before loss of accuracy occurs. These methods are called Euler-Lagrange methods by the Los Alamos school (Ref. 3).

Other uses of meshes for numerical algorithms are to reduce the trunaction errors of finite difference schemes. In other words, the mesh of fixed number of node points is adapted so as to improve the accuracy of the numerical solution. This has been the motivation of the work of Brackbill (Ref. 4), Klopfer (Ref. 5), and others. Hindman (Ref. 6) established certain properties that the transformation and the metrics must satisfy for certain mesh dependent truncation errors to vanish. He showed how these differ if the governing equations are written in various different forms, e.g., strongly and weakly conservative forms to name only two. This indicates that the form of the governing equation can also have an effect on establishing mesh criteria.

If conservation is important, as is usually the case for gas dynamics, where shock waves and tangential discontinuity surfaces are to be captured by the numerical scheme, then the mesh must be such that numerical conservation is maintained to a certain level of approximation. This requirement precludes rapid changes in mesh cell size. The changes must be smooth and gradual if conservation is required.

Another use of adaptive meshes is to keep track of fluid interfaces such flame fronts Dwyer (Ref. 7) and water waves. Here the accuracy of the solution is strongly dependent on the proper resolution of the flame front temperature gradient or air-water interface. The truncation error of the flow variables is not the problem here. The difficulty is obtaining the source terms accurately for the chemical kinetic equations or the boundary surface for the wave problem. The mesh effect on the accuracy of these flow fields will be different than those based purely on truncation errors.

Another purpose of a finite difference mesh is to control the stability, well-posedness, or convergence properties of numerical schemes. For example, Hagin (Ref. 8) used this method to keep an integral equation method well posed. Preconditioning methods or multi-grid methods also make indirect use of this mesh property to increase the convergence rate of numerical schemes Lomax (Ref. 9).

From this brief survey it is obvious that there are too many different requirements that a mesh has to satisfy. To establish criteria based on all these functions of the mesh is a far too ambitious undertaking. For this reason the remainder of this study will focus attention on meshes adapted to reduce the truncation errors only. The governing equations considered will be in strongly conservative form with no source terms due to physical processes. In the transformed or computational space the equations considered will be both strongly and weakly conservative. The source term for the latter form will be due to the transformation metrics only.

4

In the next sections the transformation, governing equations and truncation errors of a simple numerical scheme are derived.

CURVILINEAR COORDINATE SYSTEMS AND GOVERNING DIFFERENTIAL EQUATIONS

Metric Tensor

In any two dimensional surface with local coordinates $\xi^i = (\xi, \eta)$ we have a local element of length

$$ds^2 = g_{ij} d\xi^i d\xi^i \qquad\qquad i, j = 1, 2$$

$$= g_{11} d\xi^2 + 2g_{12} d\xi d\eta + g_{22} d\eta^2 \qquad\qquad (1)$$

If imbedded in a plane "physical" space with coordinates $x^i = (x, y)$ then the components of the metric tensor g_{ij} are given by

$$g_{11} = x_\xi^2 + y_\xi^2$$

$$g_{12} = x_\xi x_\eta + y_\xi y_\eta \qquad\qquad (2)$$

$$g_{22} = x_\eta^2 + y_\eta^2$$

so that $ds^2 = dx^2 + dy^2$. The determinant of the metric tensor is

$$g = |g_{ij}| = J^2 = g_{11} g_{12} - g_{12}^2 = (x_\xi y_\eta - x_\eta y_\xi)^2 \qquad\qquad (3)$$

where J is the Jacobian of the transformation between the two coordinate systems. If the mapping between the two systems is to be one-to-one, then $J \neq 0$ and $J^{-1} \neq 0$ must be satisfied.

With this transformation a mesh can be laid out with the node points at (convenient) integer values of (ξ, η). This mesh is simply a cartesian mesh with square cells and will be taken to be the computational mesh and (ξ, η) are the computational variables. The metric tensor components can be given a physican interpretation. The g_{ij} can be rewritten as

$$g_{11} = J^2 (\nabla \eta \cdot \nabla \eta)$$

$$g_{12} = J^2 (\nabla \eta \cdot \nabla \xi) \tag{4}$$

$$g_{22} = J^2 (\nabla \xi \cdot \nabla \xi) .$$

Thus g_{11} gives a measure of the length (squared) of the side of the cell parallel to the ξ coordinate, g_{22} for the length of the side parallel to the η coordinate, and g_{12} is a measure of the orthogonality between the cell sides. The metric tensor components however do not completely describe the transformation between the two spaces. The orientation of the (ξ, η) coordinate system relative to the (x, y) system is not fixed by g_{ij} and must be specified separately. One such specification can be the angle between ξ-axis and the x-axis as given by

$$\cos \phi = \frac{x_\xi}{\sqrt{x_\xi^2 + y_\xi^2}} \tag{5}$$

Other representations are possible but this one is simple and with a surface conforming curvilinear coordinate system it gives the angle between the tangent plane of the surface and the x-axis. It will be called the "solid-body" rotation angle. This solid body rotation is only defined for flat 2D surfaces. On a curved surface the integral of the rotation about a closed contour is equal to the integral of the curvature of the surface enclosed.

6

For later reference is useful to have the transformation metrics in terms of g_{ij} and ϕ.

$$x_\xi = \sqrt{g_{11}} \cos\phi$$

$$y_\xi = \sqrt{g_{11}} \sin\phi$$

$$x_\eta = \frac{-1}{\sqrt{g_{11}}} (g_{12} \cos\phi + \sqrt{g} \sin\phi)$$

(6)

and

$$y_\eta = \frac{1}{\sqrt{g_{11}}} (\sqrt{g} \cos\phi - g_{12} \sin\phi)$$

The latter two become for an orthogonal system ($g_{12} = 0$).

$$x_\eta = -\sqrt{g_{22}} \sin\phi$$

$$y_\eta = \sqrt{g_{22}} \cos\phi$$

Note the strong dependence of the metrics on the solid body rotation.

The metric tensor can be rewritten or split in various different ways. For example,

$$g_{ij} = J \begin{bmatrix} \alpha \cosh\beta & \sinh\beta \\ \sinh\beta & \frac{1}{\alpha} \cosh\beta \end{bmatrix}$$

where α is the cell aspect ratio, β is a measure of orthogonality and J the cell volume (area)

$$\alpha = \sqrt{g_{11}/g_{22}}$$

and

$$\sinh = (g_{12}/J)$$

7

Or g_{ij} can be split into dilation and shear components

$$g_{ij} = \frac{T}{2}\begin{bmatrix} 1 & 0 \\ 0 & 1 \end{bmatrix} + R\begin{bmatrix} \sin\theta & \cos\theta \\ \cos\theta & -\sin\theta \end{bmatrix}$$

where the first matrix represents a uniform dilation and the second the shear. T and R are the strength of the dilation and shear respectively. T is, of course, the trace of g_{ij}, that is

$$T = g_{11} + g_{22}$$

also

$$r = \sqrt{A^2 + B^2}$$

and

$$\sin\theta = A/\sqrt{A^2 + B^2}$$

where

$$A = (g_{11} - g_{22})/2$$

and

$$B = g_{12} .$$

With these definitions of the metric tensor, certain mesh criteria can be established.

MESH CRITERIA

In recent years curvilinear coordinate systems have become important for improving the efficiency of numerical solutions of flow fields around arbitrarily shaped bodies. In generating these meshes many workers have incorporated various properties they considered desirable into the mesh. It is not clear why these properties are required for a mesh to be "good" for a certain numerical scheme.

Brackbill (Ref. 4) generates two dimensional meshes such that several of the mesh properties are simultaneously optimized. For example, he considers cell volume, J; the trace

8

of g_{ij} which he calls cell smoothness, T; and orthogonality, g_{12} to be important. In other words he generates a mesh such that the conflicts among the three requirements are minimized. Yanenko (Ref. 10) also considers orthogonality and a specified variation of cell volume to be important. However, he does not use the cell smoothness, instead he considers a mesh "non-Lagrangian-ness" which is the difference between the fluid velocity and the mesh node velocities. Steger, et al, (Ref. 11) have developed a very rapid mesh generator by satisfying only two properties, for example, orthogonality and a simple variation of cell volume. Ablow (Ref. 12) and White (Ref. 13) use the solution in a direct manner to generate the mesh. In other words, the solution and mesh are solved simultaneously such that the measure of "difficulty" of the method is spread out uniformly over the computational domain. The "difficulty" can take on several meanings, for example, equal arc length along the solution curve, truncation error, single step error, or a number of other things. If the differential equation is the Poisson equation and one takes the truncation error to be the measure of "difficulty", then Ablow (Ref. 12) consider g_{11}, g_{12}, g_{22}, J, along with the higher order derivatives of the solution to be the important mesh criteria. Thompson (Ref. 14) have considered arc lengths between coordinate lines (i.e., g_{11} and g_{22}) and orthogonality as mesh criteria. These six works are probably the state-of-the-art in mesh generation with certain desirable properties explicitly built into them.

It should be apparent that if the mesh is solution adapted and the solution is a vector, then there should be a mesh for each component of the solution vector. This of course involves the additional expense of generating and storing multiple meshes in addition to the extra burden of interpolating among the meshes. These types of difficulties were experienced by Harlow (Ref. 1) with his "contour dynamics" method. While multiple meshes may be unnecessarily cumbersome and expensive they should

9

not be rejected out of hand for they may be advantageous for certain kinds of problems. But, in general, a single solution adapted mesh is generated based on some scalar composite of the solution vector, e.g., pressure.

It is not evident that any of these properties are in any way desirable for a "good" mesh. The very notion of a good mesh is vague. The function of any mesh network, dynamic or stationary, is to discretize a system of governing partial (usually, non-linear) differential equations so that they can be solved by a numerical algorithm. In this report only finite difference schemes will be considered. For finite difference schemes the mesh should minimize the truncation error for a given number of discretization points. This is because one can not easily add or delete mesh points during a calculation. Since the truncation error depends on the transformation metrics, the solution, and the numerical scheme, it may be expected that the desirable mesh properties will be scheme and solution dependent.

It is also possible that the mesh criteria may depend on the order of the differential equations. For this reason two types of differential equations will be considered. The first type will be a system of nonlinear first order partial differential equations, such as the Euler equations of gas dynamics. The second type will be a scalar second order partial differential equation such as the steady full potential equations for transonic flows.

<center>TRUNCATION ERROR</center>

<center>First Order Differential System -
First Order Scheme</center>

In the following sections the truncation error of two algorithms on an arbitrary curvilinear mesh will be derived. From the truncation error the desirable form of the transformation metrics will be extracted. The governing equations will be conservation law form

10

$$\overline{w}_t + \overline{f}_x + \overline{g}_y = 0 \tag{7}$$

where $\overline{f}$ and $\overline{g}$ are nonlinear functions of $\overline{w}$.

A generalized coordinate transformation is introduced

$$
\begin{aligned}
\tau &= t \\
\xi &= (t,x,y) \\
\eta &= (t,x,y)
\end{aligned} \tag{8}
$$

The transformed governing equations are written in two forms, the strong conservation law (SCL) and the weak conservation law (WCL) forms:

Strong conservation law (SCL)

$$\frac{\partial}{\partial \tau}(\overline{w}J) = \frac{\partial}{\partial \xi}\left\{y_\eta(\overline{f} - \dot{x}\overline{w}) - x_\eta(\overline{g} - \dot{y}\overline{w})\right\}$$

$$+ \frac{\partial}{\partial \eta}\left\{-y_\xi(\overline{f} - \dot{x}\overline{w}) + x_\xi(\overline{g} - \dot{y}\overline{w})\right\} = 0 \tag{9}$$

Weak conservation law (WCL)

$$\frac{\partial \overline{w}}{\partial \tau} + \frac{\partial}{\partial \xi} J^{-1}\left\{(\dot{y}x_\eta - \dot{x}y_\eta)\overline{w} + y_\eta\overline{f} - x_\eta\overline{g}\right\}$$

$$+ \frac{\partial}{\partial \tau} J^{-1}\left\{(\dot{x}y_\xi - \dot{y}x_\xi)\overline{w} - y_\xi\overline{f} + x_\xi\overline{g}\right\}$$

$$- \left\{\left[J^{-1}(\dot{y}x_\eta - \dot{x}y_\eta)\right]_\xi + \left[J^{-1}(\dot{x}y_\xi - \dot{y}x_\xi)\right]_\eta\right\}\overline{w}$$

$$- \left\{(J^{-1}y_\eta)_\xi - (J^{-1}y_\xi)_\eta\right\}\overline{f} - \left\{(-J^{-1}x_\eta)_\xi + (J^{-1}x_\xi)_\eta\right\}\overline{g} = 0 \tag{10}$$

11

To both of these forms the mesh velocities $(\dot{x}, \dot{y})$ must be given

$$
\begin{aligned}
x_\tau - \dot{x} &= 0 \\
y_\tau - \dot{y} &= 0
\end{aligned}
\tag{11}
$$

For convenience in determining the truncation error the mesh accelerations $(\ddot{x}, \ddot{y})$ are also given

$$
\begin{aligned}
(\dot{x})_\tau - \ddot{x} &= 0 \\
(\dot{y})_\tau - \ddot{y} &= 0
\end{aligned}
\tag{12}
$$

Here $\dot{x}$, $\dot{y}$, $\ddot{x}$, $\ddot{y}$ are given functions of $\overline{w}$, $\overline{w}$, $\overline{w}$, w, y.

Both of these forms are written in terms of new dependent variables and fluxes as

$$
w_\tau + f_\xi + g_\eta + h = 0
\tag{13}
$$

For the SCL form

$$
w = \begin{bmatrix} WJ \\ x \\ y \\ \dot{x} \\ \dot{y} \end{bmatrix} ; \quad
f = \begin{bmatrix} y_\eta (\overline{f} - \dot{x}\overline{w}) - x_\eta (\overline{g} - \dot{y}\overline{w}) \\ 0 \\ 0 \\ 0 \\ 0 \end{bmatrix} ;
$$

$$
g = \begin{bmatrix} -y_\xi (\overline{f} - \dot{x}\overline{w}) + x_\xi (\overline{g} - \dot{y}\overline{w}) \\ 0 \\ 0 \\ 0 \\ 0 \end{bmatrix} ; \quad
h = \begin{bmatrix} 0 \\ \dot{x} \\ \dot{y} \\ \ddot{x} \\ \ddot{y} \end{bmatrix}
\tag{14}
$$

12

and for the WCL form

$$
w = \begin{bmatrix} \overline{w} \\ x \\ y \\ \dot{x} \\ \dot{y} \end{bmatrix} \quad ; \qquad
f = \begin{bmatrix} J^{-1}\left\{ y_\eta (\overline{f} - \dot{x}\overline{w}) - x_\eta (\overline{g} - \dot{y}\overline{w}) \right\} \\ 0 \\ 0 \\ 0 \\ 0 \end{bmatrix} \quad ;
$$

$$
g = \begin{bmatrix} J^{-1}\left\{ -y_\xi (\overline{f} - \dot{x}\overline{w}) + x_\xi (\overline{g} - \dot{y}\overline{w}) \right\} \\ 0 \\ 0 \\ 0 \\ 0 \end{bmatrix} \quad ; \qquad (15)
$$

and

$$
h = \begin{bmatrix} (\text{last three terms of equation (10)} \\ \dot{x} \\ \dot{y} \\ \ddot{x} \\ \ddot{y} \end{bmatrix}
$$

Solving system (13) by a first order numerical scheme

$$
\frac{w^{n+1} - w^n}{\Delta \tau} + \frac{f^n_{i+1} - f^n_i}{\Delta \xi} + \frac{g^n_{j+1} - g^n_j}{\Delta \eta} + h^n = 0 \qquad (16)
$$

one obtains the following modified equation

$$
w_\tau + f_\xi + g_\eta + h + \frac{\Delta \tau}{2} w_{2\tau} + \frac{\Delta \xi}{2} f_{2\xi} + \frac{\Delta \eta}{2} g_{2\eta} = 0(\Delta^2)
$$

where $w_{2\tau} = w_{\tau\tau}$. This notation will be used throughout this report.

13

By eliminating $w_{2\tau}$ in terms of spatial derivatives one obtains

$$w_\tau + f_\xi + g_\eta + h + \frac{\Delta\xi}{2} f_{2\xi} + \frac{\Delta\eta}{2} g_{2\eta} + \frac{\Delta\tau}{2} (-s_\tau) = 0(\Delta^2) \qquad (17)$$

where $0(\Delta^2)$ represents $0(\Delta_\xi^2, \Delta_\eta^2, \Delta_\tau^2, \Delta_\xi\Delta_\eta)$.

Here $s = f_\xi + g_\eta + h$ and $(-s_\tau)$ is given by

$$(-s_\tau) = \Big[h_w + f_{ww_\xi} w_\xi + f_{ww_\xi} w_{\xi\xi} + f_{ww_\eta} w_{\eta\xi} + g_{ww_\eta} w_\eta + g_{ww_\xi} w_{\xi\eta}$$

$$+ g_{ww_\eta} w_{\eta\eta} \Big] \cdot s + \Big[f_w + h_{w_\xi} + f_{w_\xi w} w_\xi + f_{2w_\xi} w_{2\xi}$$

$$+ f_{w_\xi w_\eta} w_{\eta\xi} + g_{w_\xi w} w_\eta + g_{2w_\xi} w_{\xi\eta} + g_{w_\xi w_\eta} w_{2\eta} \Big] \cdot s_\xi$$

$$+ \Big[g_w + h_{w_\eta} + f_{w_\eta w} w_\xi + f_{w_\eta w_\xi} w_{\xi\xi} + f_{2w_\eta} w_{\eta\xi} + g_{w_\eta w} w_\eta$$

$$+ g_{w_\eta w_\xi} w_{\xi\eta} + g_{2w_\eta} w_{2\eta} \Big] \cdot s_\eta + \Big[h_{w_{\xi\xi}} + f_{w_\xi} \Big] \cdot s_{\xi\xi}$$

$$+ \Big[h_{w_{\xi\eta}} + f_{w_\eta} + g_{w_\xi} \Big] \cdot s_{\xi\eta} + \Big[h_{w_{\eta\eta}} + g_{w_\eta} \Big] \cdot s_{\eta\eta}$$

The meaning of these terms should be made clear. Terms with subscripts ξ or η, e.g., $s_{\xi\eta}$, are

$$s_{\xi\eta} = \frac{\partial^2}{\partial_\xi \partial_\eta}(s) = \frac{\partial^2}{\partial_\xi \partial_\eta}(f_\xi + g_\eta + h) .$$

Terms with subscripts w, w_ξ, w_η, etc. are the Jacobian coefficient matrices or flux Jacobians (not to be confused with the

14

Jacobian of the coordinate transformation). For example

$$f_{ww_\xi} = \frac{\partial^2 f}{\partial w \partial w_\xi}$$

This term is a third order tensor containing 8x8x8 terms if $\bar{w}$ is a 4-component vector as for example in the two-dimentional equations of gas dynamics.

As can be seen this modified equation is a rather complicated function of the spatial derivatives of the metrics and the flow variables. It is far too complicated for one to readily extract any useful information. It is presented, however, to emphasize the additional effects that a dynamic mesh has on the truncation error. Thus one should not be surprised by difficulties experienced with dynamic meshes as used for example by the Space Shuttle codes Kutler (Ref. 15) or the parabolized Navier-Stokes codes, Schiff (Ref. 19).

If we specialize the problem to an unsteady flow on a fixed mesh then we obtain

$$w_\tau + f_\xi + g_\eta + h + \frac{\Delta \xi}{2} f_{2\xi} + \frac{\Delta \eta}{2} g_{2\eta}$$

$$+ \frac{\Delta \tau}{2} \left[\left\{ h_w + f_{ww} w_\xi + g_{ww} w_\eta \right\} s + f_w s_\xi + g_w s_\eta \right] = 0(\Delta^2) \qquad (19)$$

Note that for this case all of the coefficient matrix Jacobians derived from the spatial derivatives of w vanish.

Comparing the two modified equations immediately reveals that the truncation error contains derivatives of one higher order for the dynamic mesh. Thus determining proper mesh criteria are more restrictive for a dynamic mesh than for a fixed mesh. If we further simplify the problem to steady flow then we obtain

15

$$f_\xi + g_\eta + h + \frac{\Delta\xi}{2}f_{2\xi} = \frac{\Delta\eta}{2}g_{2\eta} = 0(\Delta^2) \qquad (20)$$

There is no further reduction in the order of the derivative in the truncation error. The equations are recast as

$$\left[f + \frac{\Delta\xi}{2}f_\xi\right]_\xi + \left[g + \frac{\Delta\eta}{2}g_\eta\right]_\eta + h = 0(\Delta^2) \qquad (21)$$

White (Ref. 13) speaks of an ideal mesh for a one-dimensional problem as one where the numerical and exact solutions are identical. That is the truncation error vanishes. The ideal mesh for the above first order numerical scheme is one that eliminates both of the truncation errors. That is, the mesh is such that f and g are linear in ξ and η, respectively:

$$f = K_1\xi + K_2$$
$$g = K_3\eta + K_4$$

where $K_1 = -K_3 = $ constant and K_2 and K_4 are arbitrary functions of ξ and η, respectively.

For the SCL Form

$$f = y_\eta\overline{f} - x_\eta\overline{g}$$
$$g = -y_\xi\overline{f} + x_\xi\overline{g}$$

Thus a system of differential equation for x and y in terms of "known" solutions $\overline{f}$ and $\overline{g}$ is obtained.

$$\overline{f}y_\eta - \overline{g}x_\eta = K_1\xi + K_2(\xi)$$
$$-\overline{f}y_\xi + \overline{g}x_\xi = -K_1\eta + K_2(\eta)$$

16

and

$$x_\xi y_\eta - x_\eta y_\xi \neq 0 \text{ or } \neq \infty$$

This, of course, has no solutions for nontrivial $\bar{f}$ and $\bar{g}$. Thus the ideal mesh does not exist. The effect of the metrics on the truncation error can be seen by examining the truncation in expanded form. For the SCL form the errors are $\frac{\Delta\xi}{2}f_{\xi\xi}$ and $\frac{\Delta\eta}{2}g_{\eta\eta}$,

$$f_{\xi\xi} = \frac{\partial^2}{\partial\xi^2}\left[y_\eta\bar{f} - x_\eta\bar{g}\right]$$

$$= y_{\eta\xi\xi}\bar{f} - x_{\eta\xi\xi}\bar{g} + 2(y_{\eta\xi}\bar{f}_\xi - x_{\eta\xi}\bar{g}_\xi) + y_\eta\bar{f}_{\xi\xi} - x_\eta\bar{g}_{\xi\xi} \quad (22)$$

Similarly

$$g_{\eta\eta} = \frac{\partial^2}{\partial\eta^2}\left[-y_\xi\bar{f} + x_\xi\bar{g}\right]$$

$$= -y_{\xi\eta\eta}\bar{f} + x_{\xi\eta\eta}\bar{g} + 2\left(-y_{\xi\eta}\bar{f}_\eta + x_{\xi\eta}\bar{g}_\eta\right) - y_\xi\bar{f}_{\eta\eta} + x_\xi\bar{g}_{\eta\eta} \quad (23)$$

The truncation errors for the SCL form depend linearly on the metrics and their derivatives. The errors do not depend in any direct way on the Jacobian, orthogonality or cell smoothness parameters except through the metrics. They do, however, depend more directly on the solid body rotation and cell side lengths, g_{11} and g_{22} (individually, not combined into a smoothness parameter).

For the WCL form the errors are

$$f_{\xi\xi} = \frac{\partial^2}{\partial\xi^2}\left[J^{-1}\left\{y_\eta\bar{f} - x_\eta\bar{g}\right\}\right] = \left(\frac{y_\eta}{J}\right)_{\xi\xi}\bar{f} - \left(\frac{x_\eta}{J}\right)_{\xi\xi}\bar{g}$$

$$+ 2\left(\frac{y_\eta}{J}\right)_\xi\bar{f}_\xi - \left(\frac{x_\eta}{J}\right)_\xi\bar{g}_\xi + \left(\frac{y_\eta}{J}\right)\bar{f}_{\xi\xi} - \left(\frac{x_\eta}{J}\right)\bar{g}_{\xi\xi} \quad (24)$$

17

and

$$g_{\eta\eta} = \left(\frac{-y_\xi}{J}\right)_{\eta\eta} \bar{f} + \left(\frac{x_\xi}{J}\right)_{\eta\eta} \bar{g} + 2\left\{\left(\frac{-y_\xi}{J}\right)_\eta \bar{f}_\eta + \left(\frac{x_\xi}{J}\right)_\eta \bar{g}_\eta\right\}$$

$$+ \left(\frac{-y_\xi}{J}\right)\bar{f}_{\eta\eta} + \left(\frac{x_\xi}{J}\right)\bar{g}_{\eta\eta} \tag{25}$$

The errors here depend linearly on the metrics and inversely on the transformation Jacobian and their derivatives. It can be expected that the WCL forms will require meshes with smoother Jacobians than the SCL forms of the governing equations. This conclusion, of course, assumes that the metrics in the source term are computed exactly.

For both forms the mesh cell aspect ratio does not enter into the individual truncation errors. However, if the error along one coordinate line is much larger than along the other then the ratios $\frac{y_\xi}{y_\eta}$ and $\frac{x_\xi}{x_\eta}$ need not be near unity. The ratios of the metrics for an orthogonal mesh are determined by the cell aspect ratio and the solid body rotation angle.

$$\frac{y_\xi}{y_\eta} = \sqrt{\frac{g_{11}}{g_{22}}} \tan\phi$$

$$\frac{x_\xi}{x_\eta} = \sqrt{\frac{g_{11}}{g_{22}}} \frac{1}{\tan\phi}$$

Fixed mesh-unsteady flow

In this section the expanded form of equation (19) will be examined. To keep the algebra within reasonable bounds, the governing equations will be limited to the linear scalar convection equation, i.e.,

$$u_t + c_x u_x + c_y u_y = 0$$

18

where c_x and c_y are constant convection velocities in the x- and y-direction, respectively. For this example the over barred quantities corresponding to equation (7) are

$$\bar{w} = u$$

$$\bar{f} = c_x u$$

$$\bar{g} = c_y u .$$

The transformed equation is given by equation (13) and for a fixed mesh the transformed variables are for the SCL form

SCL

$$w = Ju$$

$$f = \left(\frac{c_x y_\eta}{J} - \frac{c_y x_\eta}{J}\right) Ju$$

$$g = \left(\frac{-c_x y_\xi}{J} + \frac{c_y x_\xi}{J}\right) Ju$$

and

$$h = 0$$

The flux Jacobian matrices become

$$f_w = \frac{c_x y_\eta - c_y x_\eta}{J} = \lambda$$

$$g_w = \frac{-c_x y_\xi + c_y x_\xi}{J} = \nu \qquad (26a)$$

$$f_{ww} = 0 ,$$

and

$$g_{ww} = 0 .$$

Therefore the modified equation is now

$$w_\tau + f_\xi + g_\eta + \frac{\Delta \xi}{2} f_{2_\xi} + \frac{\Delta \eta}{2} g_{2_\eta} + \frac{\Delta \tau}{2}\left\{ f_w \cdot s_\xi + g_w \cdot s_\eta \right\} = O(\Delta^2)$$

$$(26b)$$

19

where

$$s_\xi = f_{2\xi} + g_{\xi\eta}$$

and

$$s_\eta = f_{\xi\eta} + g_{2\eta}$$

In expanded form the modified equation is

$$Ju_\tau + (J\lambda)u_\xi + (J\nu)u_\eta + \frac{\Delta\xi}{2}\left\{(J\lambda)u_{2\xi} + 2(J\lambda)_\xi u_\xi + (J\lambda)_{2\xi}u\right\}$$

$$+ \frac{\Delta\eta}{2}\left\{(J\nu)u_{2\eta} + 2(J\nu)_\eta u_\eta + (J\nu)_{2\eta}u\right\} + \frac{\Delta\tau}{2}\left\{\lambda\left[(J\lambda)u_{2\xi} + (J\lambda)_\xi u_\xi\right.\right.$$

$$+ (J\nu)_\xi u_\eta\left] + \nu\left[(J\nu)u_{2\eta} + (J\nu)_\eta u_\eta + (J\lambda)_\eta u_\xi\right]\right.$$

$$+ (J\lambda)(\nu)\left[2u_{\xi\eta}\right]\right\} = 0(\Delta^2) \tag{27}$$

where λ and ν are given by equation (26a).

There are several ways this equation can be simplified for particular cases. Suppose the mesh is to be such that it induces no truncation errors when the flow is uniform. This is called the uniform free stream test by Hindman (Ref. 6). Applying the uniform free stream test u = 1 yields:

$$Ju_\tau + \frac{\Delta\xi}{2}\left\{(c_x y_\eta - c_y x_\eta)_{2\xi}\right\} + \frac{\Delta\eta}{2}\left\{(-c_x y_\xi + c_y x_\xi)_{2\eta}\right\} = 0(\Delta^2) \tag{28}$$

This equation gives the first order truncation error due to the mesh above for a uniform solution u = 1. Note that there is no mesh error with a $\Delta\tau$ dependence as all those terms cancel. This equation also gives the requirement that u = $0(\Delta^2)$, that is the metrics must be smooth enough such that

$$(c_x y_\eta - c_y x_\eta)_{2\xi} \sim 0(\Delta)$$

20

and

$$(-c_x y_\xi + c_y x_\xi)_{2\eta} \sim 0(\Delta)$$

If these conditions are not met then the free stream value of u = 1 will not be recovered to the formal order of accuracy of the numerical scheme. This uniform flow test is one method of testing the adequacy of a discretization mesh and is similar to the approach taken by Hindman (Ref. 6). Hindman's approach differs in that he tried to satisfy $u_\tau = 0$ by special differencing of the metrics for the various form of the governing equations. In the present approach the metrics are differenced no differently than the flow variables and it was only required that $u_\tau \simeq 0(\Delta^2)$ for the first order numerical scheme used.

It is quite obvious that the uniform free stream test is artificial and somewhat meaningless for a nonuniform flow field. If the flow field is uniform there is no need for the numerical scheme. As shown by equation (27) the mesh dependency of the truncation error appears in a much more complicated manner and it is somewhat difficult to separate the mesh truncation errors from those caused by the solution. This will be attempted in a later section for a second order scheme and a steady state solution.

For the WCL form of the transformed equation, the transformed variables are

WCL

$$w = u$$

$$f = \left(\frac{c_x y}{J} - \frac{c_y x}{J} \right) u$$

$$g = \left(\frac{-c_x y}{J} + \frac{c_y x}{J} \right) u$$

21

and

$$h = \left\{ \left(\frac{-y_\eta}{J} \right)_\xi + \left(\frac{y_\xi}{J} \right)_\eta \right\} c_x u + \left\{ \left(\frac{x_\eta}{J} \right)_\xi - \left(\frac{x_\xi}{J} \right)_\eta \right\} c_y u$$

The Jacobian metrices are now

$$f_w = \frac{c_x y_\eta}{J} - \frac{c_y x_\eta}{J} = \lambda$$

$$g_w = \frac{-c_x y_\xi}{J} + \frac{c_y x_\xi}{J} = \nu$$

$$h_w = h/u \qquad (u \neq 0)$$

and

$$g_{ww} = g_{ww} = h_{ww} = 0 .$$

The modified equation is now

$$w_\tau + f_\xi + g_\eta + h + \frac{\Delta\xi}{2} f_{2\xi} + \frac{\Delta\eta}{2} g_{2\eta}$$

$$+ \frac{\Delta\tau}{2} \left\{ h_w \cdot s + f_w \cdot s_\xi + g_w \cdot s_\eta \right\} = 0(\Delta^2) \qquad (29)$$

where $s = f_\xi + g_\eta + h$.

This equation may be expanded to obtain

$$u_\tau + (\lambda) u_\xi + (\nu) u_\eta + \frac{\Delta\xi}{2} \left\{ (\lambda) u_{2\xi} + 2(\lambda_\xi) u_\xi + (\lambda)_{2\xi} u \right\}$$

$$+ \frac{\Delta\eta}{2} \left\{ (\nu) u_{2\eta} + 2(\nu)_\eta u_\eta + (\nu)_{2\eta} u \right\} + \frac{\Delta\tau}{2} \left\{ \left[(\lambda^2)_\xi + (\lambda\nu)_\eta \right. \right.$$

$$+ \left. 2\lambda\frac{h}{u} \right] u_\xi + \left[(\nu^2)_\eta + (\lambda\nu)_\xi + 2\nu\frac{h}{u} \right] u_\eta + \lambda^2 u_{2\xi} + 2\lambda\nu u_{\xi\eta} + \nu^2 u_{2\eta} \right\}$$

$$= 0(\Delta^2) \qquad (30)$$

22

For the WCL form the uniform free stream test gives

$$u_\tau + \frac{\Delta\xi}{2}\left\{\frac{c_x y_\eta - c_y x_\eta}{J}\right\}_{2\xi}$$

$$+ \frac{\Delta\eta}{2}\left\{\frac{-c_x y_\xi + c_y x_\xi}{J}\right\}_{2\eta} = 0(\Delta) \tag{31}$$

This result is similar to the SCL form equation (28). The requirements for no mesh error are now

$$\left(\frac{c_x y_\eta - c_y x_\eta}{J}\right)_{2\xi} \sim 0(\Delta)$$

and

$$\left(\frac{-c_x y_\xi + c_y x_\xi}{J}\right)_{2\eta} \sim 0(\Delta) .$$

These conditions are probably more restrictive than for the SCL forms in that the Jacobian must also be smooth. These conclusions are similar to those reached by Hindman (Ref. 6). Here we conclude that the optimum mesh (optimum based, e.g., on the uniform free stream test) depends on the form of the transformed equation used. Hindman concludes that to recover the free stream values the metrics must be differenced differently depending on the form of the transformed equation solved. Of course, the mesh based on this test is not optimum in the sense of minimum truncation error of the numerical solution. For this the flow field solution and the lower order derivatives of the metrics must also be considered.

It is of interest to see how the truncation errors and thus possible mesh criteria change as a higher order numerical scheme is used to obtain the numerical solution. The derivation of the

23

modified equations both in general and expanded form for a second
order accurate leap frog scheme and system (13) have been rele-
gated to the Appendix. The major effect of the higher order
scheme can be seen by comparing the error terms of equation (A-5)
to the errors given by equations (22) and (23). The major dif-
ferences, besides the additional terms, are the appearance of
derivatives of one higher order for both the solution and the
metrics. This indicates that for higher order schemes, the
higher order derivative of the metrics must be smoother than for
a lower order scheme.

Dynamic mesh — unsteady flow

The expanded form of the modified equation for the dynamic
mesh will not be given. The algebra is nearly intractable. A
complete study of the dynamic mesh case requires the use of
machine algebra and that is beyond the scope of this study. It
is also doubtful whether anything useful in way of a solution
independent mesh criteria will evolve from such a study. It is
clear that it is not possible for the stationary mesh case covered
above.

<div align="center">Second Order Differential Equation —
Second Order Scheme</div>

In this section a scalar second order partial differential
equation solved by a simple second order accurate numerical
scheme will be examined. The steady state version of the full
potential equation for transonic flow is the model equation,
Holst (Ref. 16).

The full potential equation written in strong conservation
law form is

$$(\rho\phi_x)_x + (\rho\phi_y)_y = 0$$

$$\rho = \left[1 - \frac{\gamma-1}{\gamma+1}\left(\phi_x^2 + \phi_y^2\right)\right]^{\frac{1}{\gamma-1}} \tag{32}$$

24

where the density, ρ, and the velocity components ϕ_x, ϕ_y, are nondimensionalized with respect to the stagnation density, ρ_o, and the critical sound speed, a^*, respectively; x and y are the Cartesian coordinates and γ is the specific heat ratio.

In the transformed space [given by $\xi = \xi(x,y)$ and $\eta = \eta(x,y)$] the equation becomes

$$(J\rho U)_\xi + (J\rho V)_\eta = 0 \tag{33}$$

where

$$U = (g_{22}\phi_\xi - g_{12}\phi_\eta)/J^2$$

$$V = (-g_{12}\phi_\xi + g_{11}\phi_\eta)/J^2$$

The definitions of g_{11}, g_{12}, g_{22}, and J are given by equations (2) and (3). The density is now

$$\rho = \left[1\left[-\frac{\gamma-1}{\gamma+1}\left\{\left(\frac{g_{22}}{J^2}\right)\phi_\xi^2 - 2\left(\frac{g_{12}}{J^2}\right)\phi_\xi\phi_\eta + \left(\frac{g_{11}}{J^2}\right)\phi_\eta^2\right\}\right]\right]^{\frac{1}{\gamma-1}} \tag{34}$$

It should be noted that for this second order differential equation that the "traditional" mesh criteria reappear directly, namely, J, g_{11}, g_{22}, and g_{12}. This is unlike a first order differential system where only the metrics and J appear.

Since for full potential equations the density is usually the desired solution from which the pressure and Mach numbers can be determined we will examine the truncation error of equation (34) only. For simplicity simple central differencing will be used throughout the entire flow field whether the local Mach numbers are sub- or supersonic. Let the "exact" density be given by ρ_E and the numerically derived density by ρ_N. The relation between the two is

$$\rho_E = \rho_N + \Delta\rho + \text{higher order terms}$$

$$\cong \rho_N\left(1 + \frac{\Delta\rho}{\rho_N}\right)$$

The $\Delta\rho$ can be derived from the modified equation form of equation (34). Replacing all the derivatives by central differences and expanding in a Taylor series obtains the modified equation of (34) as

$$\rho_E \cong \rho_N - \frac{1}{\gamma + 1}\left\{\frac{g_{22}}{J^2}\Delta\left(\phi_\xi^2\right) - \frac{2g_{12}}{J^2}\Delta\left(\phi_\xi\phi_\eta\right) + \frac{g_{11}}{J^2}\Delta\left(\phi_\eta^2\right)\right\}$$

$$- \frac{1}{\gamma + 1}\left\{\phi_\xi^2\Delta\left(\frac{g_{22}}{J^2}\right) - 2\phi_\xi\phi_\nu\Delta\left(\frac{g_{12}}{J^2}\right) + \phi_\eta^2\Delta\left(\frac{g_{11}}{J^2}\right)\right\} \qquad (35)$$

where

$$\Delta\left(\phi_\xi^2\right) = \frac{\Delta\xi^2}{3}\phi_\xi\phi_{3\xi}$$

$$\Delta\left(\phi_\xi\phi_\eta\right) = \frac{\Delta\eta^2}{6}\phi_\xi\phi_{3\eta} + \frac{\Delta\xi^2}{6}\phi_\eta\phi_{3\xi}$$

$$\Delta\left(\phi_\eta^2\right) = \frac{\Delta\eta^2}{3}\phi_\eta\phi_{3\eta}$$

$$\Delta\left(\frac{g_{22}}{J^2}\right) = \frac{\Delta\eta^2}{3}\left(\frac{x_\eta x_{3\eta} + y_\eta y_{3\eta}}{J^2}\right) - \frac{g_{22}}{3J^3}\Delta J$$

$$\Delta\left(\frac{g_{12}}{J^2}\right) = \frac{\Delta\eta^2}{6}\left(\frac{x_\xi x_{3\eta} + y_\xi y_{3\eta}}{J^2}\right) + \frac{\Delta\xi^2}{6}\left(\frac{x_\eta x_{3\xi} + y_\eta y_{3\xi}}{J^2}\right) - \frac{g_{12}}{3J^3}\Delta J$$

26

$$\Delta\left(\frac{g_{12}}{J^2}\right) = \frac{\Delta\xi^2}{3}\left(\frac{x_\xi x_{3\xi} + y_\xi y_{3\xi}}{J^2}\right) - \frac{g_{11}}{3J^3}\Delta J$$

and

$$\Delta J = \Delta\eta^2(x_\xi y_{3\eta} - y_\xi x_{3\eta}) + \Delta\xi^2(y_\eta x_{3\xi} - x_\eta y_{3\xi}) .$$

Note that the effect of the truncation errors of the metrics and the solution (ϕ) are somewhat separable. In equation (35) the first group of terms on the right hand side is the truncation due to the solution. This part of the error still has the metrics as coefficients. The second group of terms is the mesh induced truncation error and also depends on the solution. Only in this sense are the two errors separable. Thus, for a given solution one could check the adequacy of a mesh by computing the two separate errors as above and require that the mesh induced errors be no larger than the solution induced errors over the entire solution domain.

This is not a very satisfactory result in that a mesh induced truncation error only has meaning with respect to a particular flow field solution. A numerical example for the full potential equation is presented in a later section.

MESH-INDUCED NUMERICAL INSTABILITY

The use of curvilinear mesh or a nonuniform Cartesian mesh can introduce what will be called mesh-induced numerical instability. Although a numerical scheme may be stable for a uniform Cartesian mesh, there is no guarantee it will remain stable on another type of mesh. This assertion can be quickly verified by examining the modified equation (A-5). In this equation there are four dissipative terms whose coefficients depend on the local metrics and their derivatives. These four terms are

$$\frac{\Delta\xi^2}{3!}\left(3y_{\eta\xi}\overline{f}_{2\xi}\right)$$

$$\frac{\Delta\xi^2}{3!}\left(-3x_{\eta\xi}\overline{g}_{2\xi}\right)$$

$$\frac{\Delta\eta^2}{3!}\left(-3y_{\xi\eta}\overline{f}_{2\eta}\right)$$

and

$$\frac{\Delta\eta^2}{3!}\left(3x_{\xi\eta}\overline{g}_{2\eta}\right).$$

These terms can act as either damping or destabilizing terms depending on the signs of $x_{\xi\eta}$ and $y_{\xi\eta}$. If they are destabilizing, then they must be stabilized by either the inherent dissipation of the scheme (which the leap frog scheme does not have) or by the artificial dissipation usually appended .o the scheme. In some cases for which the metrics vary rapidly enough, the numerical or artificial dissipation may not be sufficient and thus a mesh induced instability can occur. An example of this occurrence has been shown by Hindman (Ref. 6).

This unpleasant problem does not occur for uniform Cartesian meshes and no solution is offered here. We simply wish to raise a warning flag that even though a mesh is generated according to some criteria based on truncation errors there is no guarantee that the numerical scheme will be stable.

NUMERICAL RESULTS

Some numerical results will be presented here. The results will be in terms of a post-mortem. For a given mesh and numerical solution based on the full potential code (Holst, Ref. 16) as modified by Dougherty (Ref. 17) the truncation errors will be analyzed to see if the mesh indeed was adequate.

The grid is shown in Figure 1. Shown is a C-type mesh around a NACA 0012 airfoil. The far field boundaries (not shown) are approximately six chord lengths from the airfoil in all directions. It consists of 175 × 31 node points and is generated by use of the Poisson equation with some grid control (Sorenson, Ref. 18). A solution in terms of density is shown in Figures 2 and 3 for a free stream Mach number $M_\infty = 0.80$ and angle of attack $\alpha = 0°$. These results are presented as carpet plots with the computational variables I, J (representing ξ, η, respectively) as the independent variables. The airfoil surface is given by $J = 31$ and the far field boundary by $J = 1$. The leading edge of the airfoil at $I = 88$ and the trailing edge at $I = 31$. The plots are distorted but this should cause no confusion. The viewpoint of Figure 2 is thus at the far field boundary and the leading edge. In other words, from the right hand side of Figure 1. The viewpoint of Figure 3 and all the subsequent figures is from the far field boundary and the trailing edge, or the lower left hand corner of Figure 1. The rise of the density at the leading edge stagnation point and at the shock wave is quite apparent.

The next set of three figures presents some of the traditional mesh criteria. These are the smoothness $(g_{11} + g_{22})$ in Figure 4, the Jacobian (plotted inversely) in Figure 5, and the orthogonality $(g_{12}$, labelled as "skew") in Figure 6. The plots have all been normalized with the normalization constants shown on the plots. These figures show that the smoothness parameter is very uniform near the airfoil and becoming less so at the far field boundary. The Jacobian plot, Figure 5, indicates that most of the variation occurs near the leading edge and relatively little elsewhere. The mesh is nearly orthogonal except at the trailing edge and far field boundary, as shown by Figure 6.

Figures 7 and 8 present the variations of g_{11} and g_{22}. As shown they are nearly uniform except at the trailing edge and far field boundary, with g_{22} being an order of magnitude more

important (its normalization factor is 10 times larger). The solid body rotation, $\cos\phi$, is shown in Figure 9 and is labelled as ROTAT. The cell aspect ratio, $\sqrt{g_{11}/g_{22}}$, labelled ASPECT, is given in the following figure. Both of these indicate large variations near the trailing edge and the leading edge.

The following set of four figures present the metrics directly. These are y_η, x_η, y_ξ, and x_ξ in Figures 11, 12, 13, and 14, respectively. These figures indicate that the largest variations of the metrics occur near the trailing edge and at the far field boundary. They are quite uniform near the leading edge. This indicates that the mesh has been sufficiently re-fined there to reduce the solid body angle variation to accept-able levels. It may be possible, however, that the extra resolution is needed to resolve the peak of stagnation density adequately.

Based on these results one would expect most of the mesh induced truncation errors to occur near the trailing edge and at the far field boundary. That this is indeed the case is con-firmed in Figure 15. Shown here is the second group of terms of equation (35) in terms of percentage of ρ_N (the numerically computed density). The mesh induced errors occur mostly near the trailing edge and the far field boundary. They are on the order of 2 to 3%.

The solution induced truncation error [first group of terms of equation (35)] is shown in Figure 16. These errors are much larger. They are on the order of 1-2% near the leading edge, 5% at the shock wave, <5% at the trailing edge, and 2% at the far field. The total error is shown in Figure 17. As can be seen some of the errors at the trailing edge and far field have been cancelled. This is, however, a fortuitous circumstance and, in general, should not be expected to occur. The errors are still approximately 2% at the leading and trailing edges and 5% at the shock wave.

30

One concludes that the mesh of Figure 1 is probably more than adequate for controlling the mesh induced errors, if 5% solution errors are acceptable. If drag calculations are to be attempted with this mesh and numerical procedure, then 2% accuracy at the trailing and leading edge is probably not acceptable. The errors would need to be reduced by further mesh refinement.

RECOMMENDATIONS

Based on the results of this study the following recommendations are offered:

1) Generate a mesh based on acceptable variations of either

a) x_ξ, y_η, x_η, y_ξ for first order differential systems, or

b) g_{11}, g_{22}, g_{12}, $\cos\phi$ for second order differential systems.

Acceptable variations can be checked by plots made as shown by Figures 4 through 11.

2) Once the converged numerical solution has been obtained (hopefully the scheme is still stable) do the truncation error analysis and numerically compute the mesh and solution induced truncation errors. If these are not at acceptable levels, then a new mesh needs to be generated until acceptable error levels are obtained. (It should be standard practice for any numerical computation that the truncation errors are also computed.)

3) For higher numerical schemes the variations of the mesh criteria must be less than for lower order schemes.

4) For dynamic meshes the variations of the mesh criteria must again be less than for stationary schemes.

EXTENSION TO THREE-DIMENSIONS

The extensions of the above results is straight forward in the sense that one can readily identify the additional parameters

31

that can make up the mesh criteria. For the 3-D systems, there
are six components to the metric tensor, i.e.,

$$ds^2 = g_{ij}d\xi^i d\xi^i \qquad\qquad i,j = 1,2,3$$

$$= g_{11}d\xi^2 + 2g_{12}d\xi d\eta + 2g_{13}d\xi d\zeta$$

$$+ 2g_{23}d\eta d\zeta + g_{22}d\eta^2 + g_{33}d\zeta^2$$

and there are nine metric terms, i.e.

$$\frac{\partial(x,y,z)}{\partial(\xi,\eta,\zeta)} = \begin{bmatrix} x_\xi & x_\eta & x_\zeta \\ y_\xi & y_\eta & y_\zeta \\ z_\xi & z_\eta & z_\zeta \end{bmatrix}$$

If the metric tensors are used as the mesh criteria, then
three solid body rotation angles need to be included to completely
describe the mesh properties.

While the additional elements for the 3-D case are obvious,
deriving the truncation errors is probably impossible to do by
hand. The use of machine algebra would be mandatory.

CONCLUSIONS

In this study an attempt has been made to establish some
criteria for generating finite difference grids. However, it
has been shown by truncation error analysis that it is not pos-
sible to do so independently of the numerical solution obtained
on the mesh. The study has been limited to mesh criteria which
reduce the truncation errors. These truncation errors depend on
the order of the differential system, the solution, the form of
the transformed equation, the order and type of numerical scheme,

32

and the mesh itself. The results of this study show that probably the best strategy is to follow the procedure given in the recommendations section. The mesh cannot be judged by itself. Its use must also be considered.

APPENDIX A

In this appendix the modified equation for a higher order numerical solution to the system of equations (13) is derived. The numerican scheme is the leap frog scheme. Although this scheme is in general unstable, it is second order accurate both spatially and temporarily, and thus is represents a typical second order scheme. It is much simpler to analyze than say MacCormack's scheme.

The leap frog scheme is given by

$$\frac{w^{n+1} - w^{n-1}}{2\Delta\tau} + \frac{f^n_{i+1} - f^n_{i-1}}{2\Delta\xi} + \frac{g^n_{j+1} - g^n_{i-1}}{2\Delta\eta} + h = 0 \qquad (A-1)$$

The modified equation for this scheme and system (13) is

$$w_\tau + f_\xi + g_\eta + h + \frac{\Delta\tau}{3!}w_{3\tau} + \frac{\Delta\xi}{3!}f_{3\xi} + \frac{\Delta\eta}{3!}g_{3\eta} = O(\Delta^4)$$

Eliminating the higher order time derivatives obtains, after considerable algebra, the final modified equation.

$$w_\tau + \frac{\partial}{\partial\xi}\left[f + \frac{\Delta\xi^2}{3!}f_{2\xi}\right] + \frac{\partial}{\partial\eta}\left[g + \frac{\Delta\eta^2}{3!}g_{2\eta}\right] + h - \frac{\Delta\tau^2}{3!}\frac{\partial}{\partial\xi}\left[f_{2w}s \cdot s \right.$$

$$+ f_{2w_\xi}s_\xi \cdot s_\xi + f_{2w_\eta}s_\eta \cdot s_\eta + 2f_{ww_\xi}s_\xi \cdot s + 2f_{ww_\eta}s_\eta \cdot s$$

$$\left. + 2f_{w_\xi w_\eta}s_\eta \cdot s_\xi + f_w(-s_\tau) + f_{w_\xi}(-s_{\tau\xi}) + f_{w_\eta}(-s_{\tau\eta})\right]$$

$$- \frac{\Delta\tau^2}{3!}\frac{\partial}{\partial\eta}\left[g_{2w}s \cdot s + g_{2w_\xi}s_\xi \cdot s_\xi + g_{2w_\eta}s_\eta \cdot \varepsilon_\eta + 2g_{ww_\xi}s_\xi \cdot s \right.$$

(Continued on next page)

$$+ 2g_{ww_\eta} s_\eta \cdot s + 2g_{w_\xi w_\eta} s_\eta \cdot s_\xi + g_w(-s_\tau) + g_{w_\xi}(-s_{\tau\xi}) + g_{w_\eta}(-s_{\tau\eta}) \Big]$$

$$- \frac{\Delta\tau^2}{3!}\Big[h_w(-s_\tau) + h_{w_\xi}(-s_{\tau\xi}) + h_{w_\eta}(-s_{\tau\eta}) + h_{w_{\xi\xi}}(-s_{\tau\xi\xi})$$

$$+ g_{w_{\xi\eta}}(-s_{\tau\xi\eta}) + h_{w_{\eta\eta}}(-s_{\tau\eta\eta}) \Big] - \frac{\Delta\tau^2}{3!}\Big[h_{2w} s \cdot s + h_{2w_\xi} s_\xi \cdot s_\xi$$

$$+ h_{2w_\eta} s_\eta \cdot s_\eta + 2h_{ww_\xi} s_\xi \cdot s + 2h_{ww_\eta} s_\eta \cdot s + 2h_{w_\xi w_\eta} s_\xi \cdot s_\eta$$

$$+ h_{ww_{\xi\xi}} s \cdot s_{\xi\xi} + h_{w_\xi w_{\xi\xi}} s_\xi \cdot s_{\xi\xi} + h_{w_\eta w_{\xi\xi}} s_\eta \cdot s_{\xi\xi} + h_{ww_{\xi\eta}} s \cdot s_{\xi\eta}$$

$$+ h_{w_\xi w_{\xi\eta}} s_\xi \cdot s_{\xi\eta} + h_{w_\eta w_{\xi\eta}} s_\eta \cdot s_{\xi\eta} + h_{ww_{\eta\eta}} s_\eta \cdot s_{\eta\eta} + h_{w_\xi w_{\eta\eta}} s_\xi \cdot s_{\eta\eta}$$

$$+ h_{w_\eta w_{\eta\eta}} s_\eta \cdot s_{\eta\eta} \Big] = 0(\Delta^4) \tag{A-2}$$

where

$$s = f_\xi + g_\eta + h$$

and

$$-s_\tau = \frac{\partial}{\partial\xi}\Big[f_w s + f_{w_\xi} s_\xi + f_{w_\eta} s_\eta \Big]$$

$$+ \frac{\partial}{\partial\eta}\Big[g_w s + g_{w_\xi} s_\xi + g_{w_\eta} s_\eta \Big]$$

$$+ h_w s + h_{w_\xi} s_\xi + h_{w_\eta} s_\eta + h_{w_{\xi\xi}} s_{\xi\xi}$$

$$+ h_{w_{\xi\eta}} s_{\xi\eta} + h_{w_{\eta\eta}} s_{\eta\eta}$$

36

The following observations are made:

1. The time dependent part makes an awful mess of the situation. We may want to consider steady solution first. But they also show why adaptive meshes can slow convergence to steady state and cause other difficulties.

2. There are several flux Jacobian metrices, i.e.,

$$f_w, \quad f_{w_\xi}, \quad f_{w_\eta}, \quad g_w, \quad g_{w_\xi}, \quad g_{w_\eta}$$
$$h_w, \quad h_{w_\xi}, \quad h_{w_\eta}, \quad h_{w_{\xi\xi}}, \quad h_{w_{\xi\eta}}, \quad h_{w_{\eta\eta}}$$

and the higher order Jacobians.

The terms involving $\frac{\partial}{\partial w}$ are due to the solution, those involving $\frac{\partial}{\partial w_\xi}$ etc. are due the metrics (i.e., mesh). The terms involving both (with the higher order Jacobians) are due to both the solution and the metrics.

3. The terms involving s contain the effects of both the solution and the mesh.

4. The observations made for the first order scheme apply here also.

To simplify the modified equation to a reasonable level assume that the mesh is fixed with time, but still consider time variations of the solution. In this case the modified equation reduces to

$$w_\tau + \frac{\partial}{\partial \xi}\left[f + \frac{2}{3!}f_{2\xi}\right] + \frac{\partial}{\partial \eta}\left[g + \frac{2}{3!}g_{2\eta}\right] + h - \frac{\Delta\tau^2}{3!}\frac{\partial}{\partial \xi}\left[f_{2w}s \cdot s\right.$$

$$\left. + f_w(-s_\tau)\right] - \frac{\Delta\tau^2}{3!}\frac{\partial}{\partial \eta}\left[g_{2w}s \cdot s + g_w(-s_\tau)\right] - \frac{\Delta\tau^2}{3!}\left[h_{2w}s \cdot s\right.$$

$$\left. + h_w(-s_\tau)\right] = 0(\Delta^4) \tag{A-3}$$

where

$$s = f_\xi + g_\eta + h$$

and

$$-s_\tau = \frac{\partial}{\partial \xi}\left[f_w \cdot s\right] + \frac{\partial}{\partial \eta}\left[g_w \cdot s\right] + h_w \cdot s$$

The modified equation for the leap frog scheme on a fixed mesh given above is similar to that of the first order scheme, equation (19). The truncation errors are of course of one higher order. Thus it can be concluded that the higher order derivatives of the meshes must be smoother for higher order schemes than for lower order schemes. To see this consider the steady state form of equation (A-3).

$$f_\xi + g_\eta + h + \frac{\Delta\xi^2}{3!}f_{3\xi} + \frac{\Delta\eta^2}{3!}g_{3\eta} = 0(\Delta^4) \tag{A-4}$$

Now need to specialize this modified equation to either the SCL or WCL form. Doing the SCL form first.

SCL

$$w = \frac{w}{J}$$

$$f = y_\eta \bar{f} - x_\eta \bar{g}$$

$$g = -y_\xi \bar{f} + x_\xi \bar{g}$$

$$h = 0 .$$

$$\left(y_\eta \overline{f} - x_\eta \overline{g}\right)_\xi + \left(-y_\xi \overline{f} + x_\xi \overline{g}\right)_\eta + \frac{\nabla \xi^2}{3!}\left\{y_{\eta 3\xi}\overline{f} - x_{\eta 3\xi}\overline{g} + 3y_{\eta 2\xi}\overline{f}_\xi\right.$$

$$- 3x_{\eta 2\xi}\overline{g}_\xi + 3y_{\eta\xi}\overline{f}_{2\xi} - 3x_{\eta\xi}\overline{g}_{2\xi} + y_\eta \overline{f}_{3\xi} - x_\eta \overline{g}_{3\xi}\left.\right\}$$

$$+ \frac{\Delta \eta^2}{3!}\left\{-y_{\xi 3\eta}\overline{f} + x_{\xi 3\eta}\overline{g} - 3y_{\xi 2\eta}\overline{f}_\eta + 3x_{\xi 2\eta}\overline{g}_\eta - 3y_{\xi\eta}\overline{f}_{2\eta} + 3x_{\xi\eta}\overline{g}_{2\eta}\right.$$

$$- y_\xi \overline{f}_{3\eta} + x_\xi \overline{g}_{3\eta}\left.\right\} = 0(\Delta^4) \tag{A-5}$$

The error terms of this equation should be compared with the first order scheme error terms given by equations (22) and (23). Similar results are obtained for the WCL form of the transformed equations.

<u>WCL</u>

$$w = \overline{w}$$

$$f = J^{-1}(y_\eta \overline{f} - x_\eta \overline{g})$$

$$g = J^{-1}(-y_\xi \overline{f} + x_\xi \overline{g})$$

$$h = -\left[(J^{-1}y_\eta)_\xi - (J^{-1}y_\xi)_\eta\right]f$$

$$\qquad -\left[-(J^{-1}x_\eta)_\xi + (J^{-1}x_\xi)_\eta\right]g$$

The WCL modified equation becomes

$$\left[J^{-1}\left(y_\eta \overline{f} - x_\eta \overline{g}\right)\right]_\xi + \left[J^{-1}\left(-y_\xi \overline{f} + x_\xi \overline{g}\right)\right]_\eta + h$$

$$+ \frac{\Delta\xi^2}{3!}\left\{\left(J^{-1}y_n\right)_{3\xi}\bar{f} - \left(J^{-1}x_n\right)_{3\xi}\bar{g} + 3\left(J^{-1}y_n\right)_{2\xi}\bar{f}_\xi - 3\left(J^{-1}x_n\right)_{2\xi}\bar{g}_\xi\right.$$

$$\left. + 3\left(J^{-1}y_n\right)_\xi\bar{f}_{2\xi} - 3\left(J^{-1}x_n\right)_\xi\bar{g}_{2\xi} + \left(J^{-1}y_n\right)\bar{f}_{3\xi} - \left(J^{-1}x_n\right)\bar{g}_{3\xi}\right\}$$

$$+ \frac{\Delta\eta^2}{3!}\left\{\left(-J^{-1}y_\xi\right)_{3\xi}\bar{f} + \left(J^{-1}x_\xi\right)_{3\eta}\bar{g} + 3\left(-J^{-1}y_\xi\right)_{2\eta}\bar{f}_\eta + 3\left(J^{-1}x_\xi\right)_{2\eta}\bar{g}_\eta\right.$$

$$\left. + 3\left(-J^{-1}y_\xi\right)_\eta\bar{f}_{2\eta} + \left(J^{-1}x_\xi\right)_\eta\bar{g}_{2\eta} + \left(-J^{-1}y_\xi\right)\bar{f}_{3\eta} + \left(J^{-1}x_\xi\right)\bar{g}_{3\eta}\right\}$$

$$= 0(\Delta^4) \hspace{4cm} \text{(A-6)}$$

where

$$J^{-1} = \frac{1}{x_\xi y_\eta - x_\xi y_\eta}$$

The error terms of this equation should be compared with the first order scheme error terms given by equations (24) and (25).

. REFERENCES

1. Harlow, F.H.: Contour Dynamics for Numerical Fluid Flow Calculations, JCP Vol. 8, 214-229, 1971.

2. Klopfer, G.H.: Lagrangian Computation of Inviscid Compressible Flows, NASA TMS-78456, 1978.

3. Hirt, C.W. and Cook, J.L.: Calculating Three-Dimensional Flows Around Structures and over Rough Terrain, JCP Vol. 10, 324, 1972.

4. Brackbill, J.O. and Saltzman, J.S.: Adaptive Zoning for Singular Problems in Two Dimensions, Los Alamos Scientific Laboratory, LA-UR-81-405, 1981 (submitted to JCP).

5. Klopfer, G.H. and McRae, D.A.: The Nonlinear Truncation Error Analysis Approach to Analyzing Finite Difference Schemes, AIAA Paper 81-1029, 5th AIAA CFD Conference, Palo Alto, California, 1981.

6. Hindman, R.G.: Geometrically Induced Errors and Their Relationship to the Form of the Governing Equations and the Treatment of Generalized Mappings, AIAA Paper 81-1008, 5th AIAA CFD Conference, Palo Alto, California, 1981.

7. Dwyer, H.A., Kee, R.J., and Sanders, B.R.: Adaptive Grid Method for Problems in Fluid Mechanics and Heat Transfer, AIAA Jour. Vol. 18, No. 10, pp. 1205-1212, October 1980.

8. Hagin, F.: On the Construction of Well-Conditioned Systems for Fredholm I Problems by Mesh Adapting, JCP Vol. 36, No. 2, pp. 154-169, 1980.

9. Lomax, H., Pulliam, T., and Jespersen J.: Eigen System Analysis Techniques for Finite Difference Equation I Multilevel Techniques. AIAA Paper 81-1027, 5th AIAA CFD Conference, Palo Alto, California, 1981.

10. Yanenko, N.N., Kroshko, E.A., Liseikin, V.V., Fomin, V.M., Shapero, V.P., and Shapeev, Y.A.: Methods for the Construction of Moving Grids for Problems of Fluid Dynamics with Big Deformations, Proceedings of the 5th International Conference on Numerical Methods in Fluid Dynamics, Lecture notes in Physics, Vol. 59, Springer-Verlag, 1976.

11. Steger, J.L. and Chaussee, D.S.: Generation of Body Fitted Coordinates Using Hyperbolic Partial Differential Equations, Flow Simulations, Inc., Report 80-1, 1980.

REFERENCES (Concluded)

12. Ablow, C.M. and Schechter, S.: Generation of Boundary and Boundary-Layer Fitting Grids, NASA Conference Publications 2166, 1980.

13. White, A.: Computational Experiences with Some Mesh Selection Techniques, Adaptive Mesh Workshop, Los Alamos, New Mexico, 1981.

14. Thompson, J.F. and Gastin, C.W.: Grid Generation Using Differential Systems Techniques, NASA Conference Publications 2166, 1980.

15. Kutler, P., Reinhardt, W.A., and Warming, R.F.: Multishocked, Three-Dimensional Supersonic Flowfields with Real Gas Effects, AIAA Jour., Vol. 11, No. 5, pp. 657-664, 1973.

16. Holst, T.L.: An Implicit Algorithm for the Conservative, Transonic Full Potential Equation Using an Arbitrary Mesh, AIAA J. Vol. 17, Oct., pp. 1038-1056, 1979.

17. Dougherty, F.C.: TAIRC Code, in preparation, NASA Ames Research Center, 1982.

18. Sorenson, R.L. and Steger, J.L.: Numerical Generation of Two-Dimensional Grids by the Use of Poisson Equations with Grid Control at Boundaries, NASA Conference Publications 2166, 1980.

19. Schiff, L.B. and Steger, J.L.: Numerical Simulation of Steady Supersonic Viscous Flow, AIAA Paper 79-0130, Aerospace Sciences Meeting, New Orleans, Louisana, 1979.

42
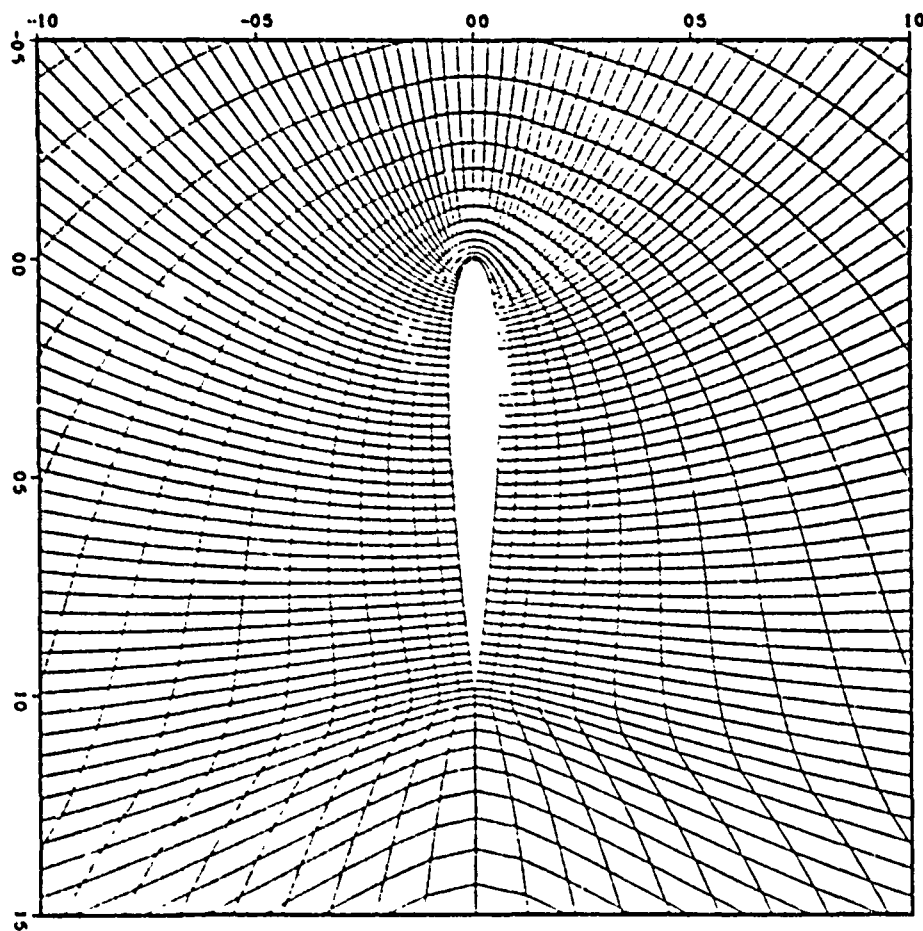
Figure 1. Grid plot of a C-mesh around a NACA 0012 airfoil — 175 x 31 mesh points.

43
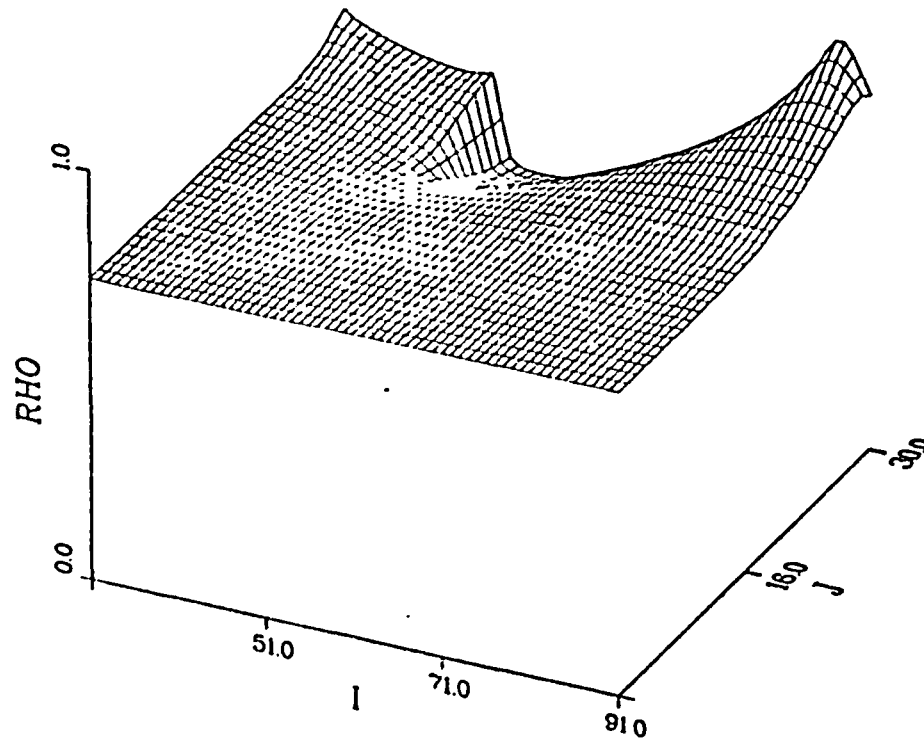
Figure 2.   Carpet plot of density solution as solved by TAIRC (ref.17) on lower
half of NASA 0012 airfoil, $M_\infty = 0.80$, $\alpha = 0°$.

Viewpoint is from leading edge.
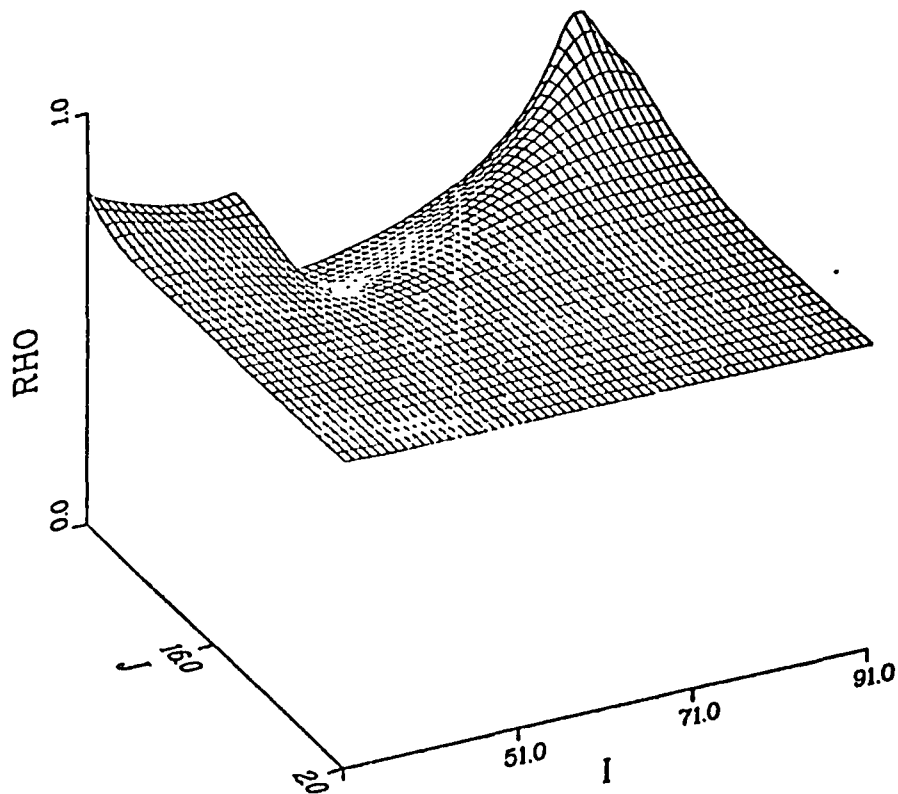
Figure 3.   Carpet plot of density solution as solved by TAIRC (ref. 17) on lower
half of NACA 0012 airfoil, $M_\infty = 0.80$, $\alpha = 0°$.   Viewpoint from
near the trailing edge and far field boundary
(lower left hand corner of figure 1.)
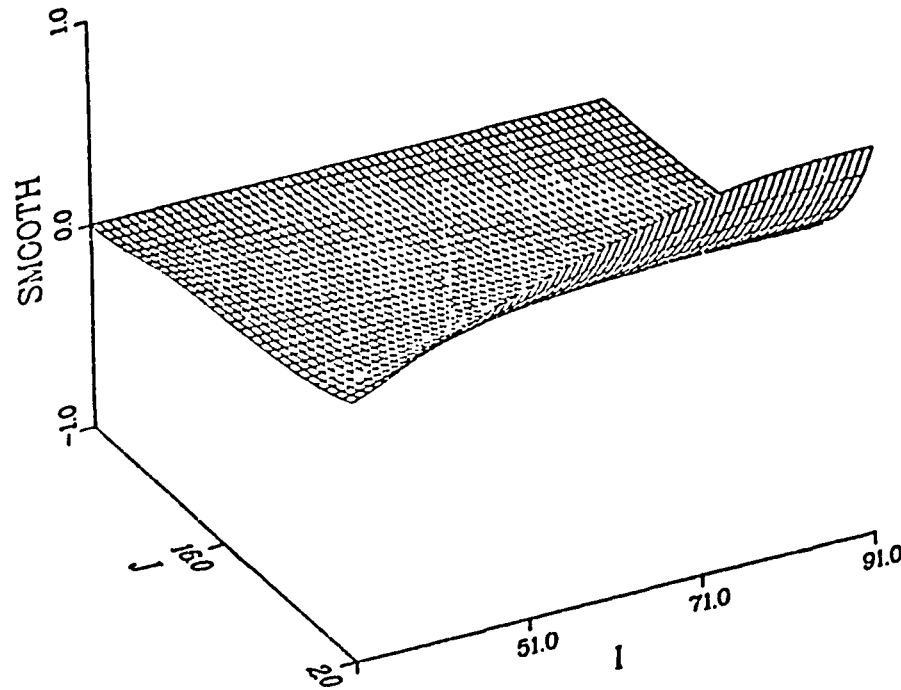
Figure 4.   Carpet plot of the smoothness parameter $(g_{11} + g_{12})$ normalized by 0.4741.
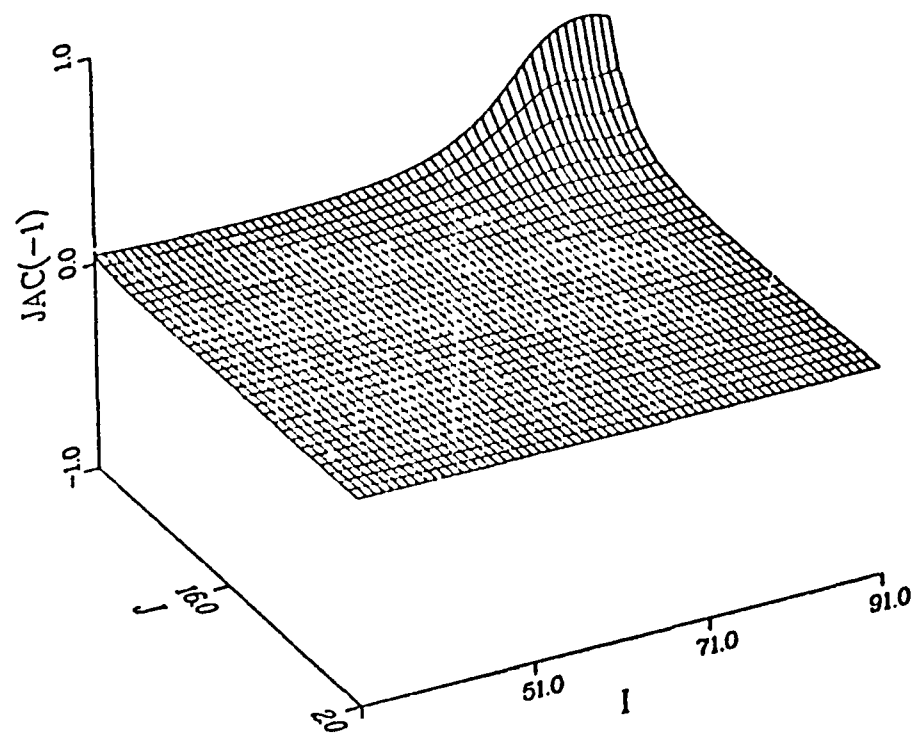
Figure 5. Carpet plot of the inverse of the transformation
Jacobian normalized by 32460.
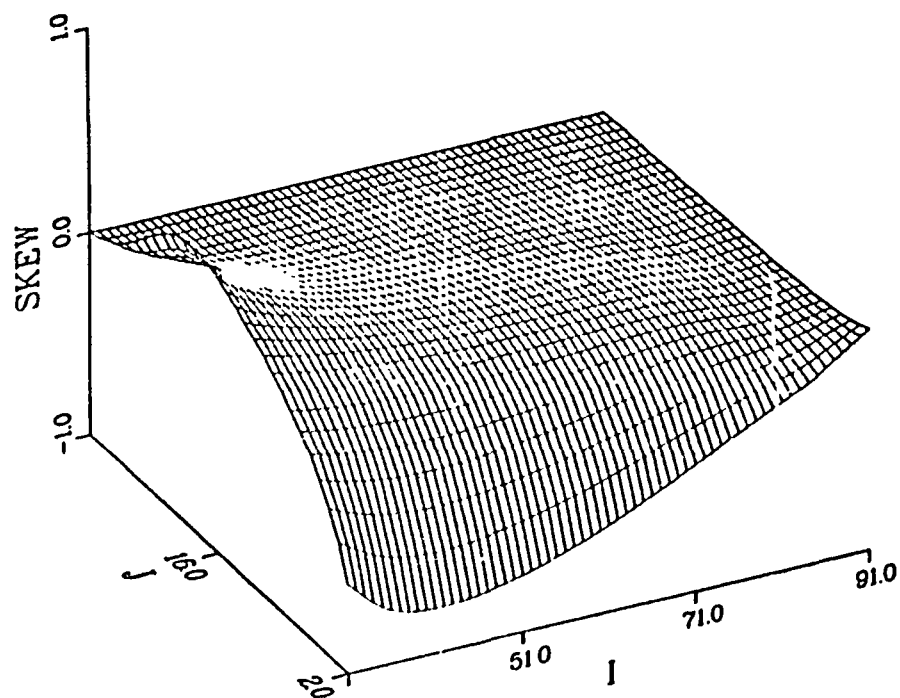
Figure 6. Carpet plot of the orthogonality parameter (g_{12})
normalized by 0.02797.
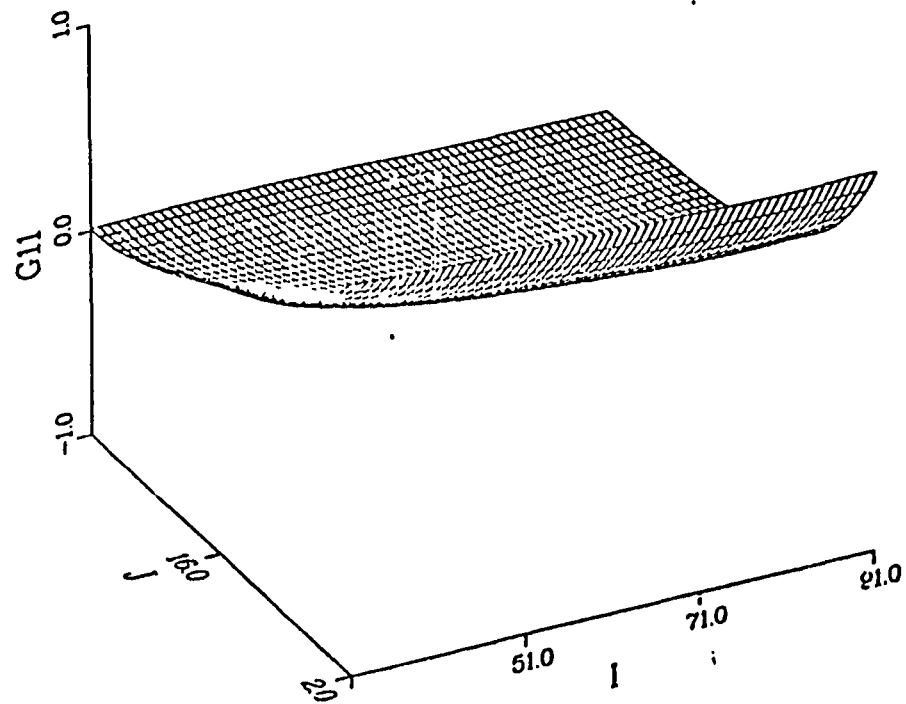
Figure 7. Carpet plot of length parameter g_{11} normalized by 0.03143.
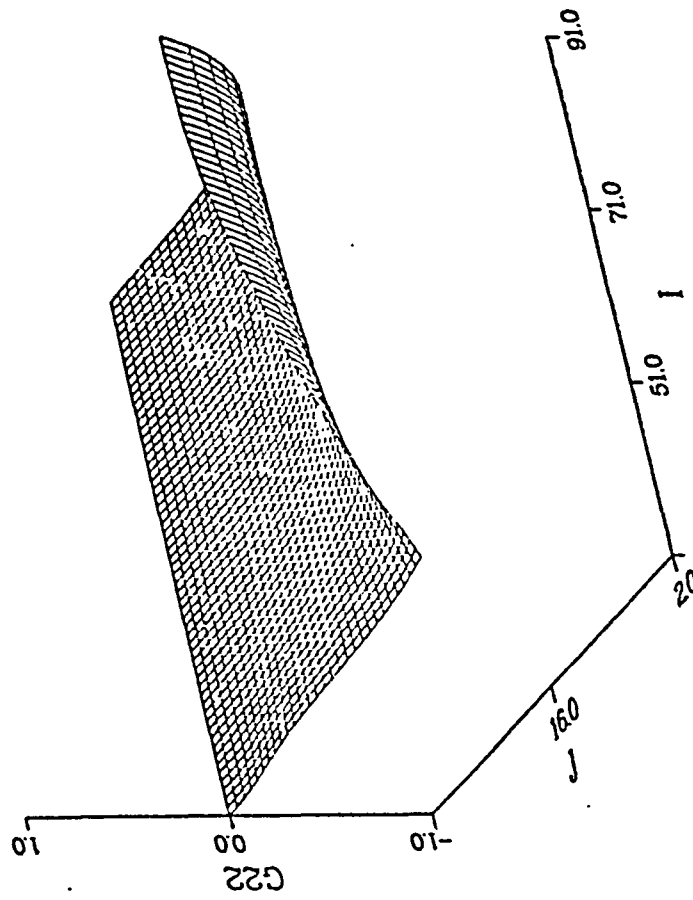
Figure 8. Carpet plot of length parameter g_{22} normalized by 0.4427.
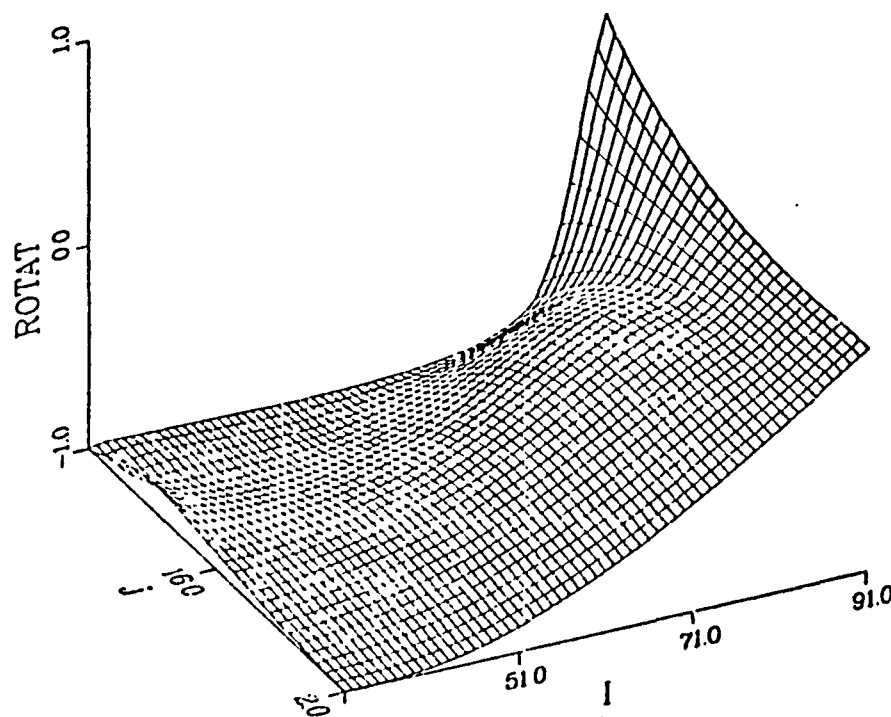
Figure 9. Carpet plot of solid body rotation parameter $\cos\phi$ normalized by 1.00.
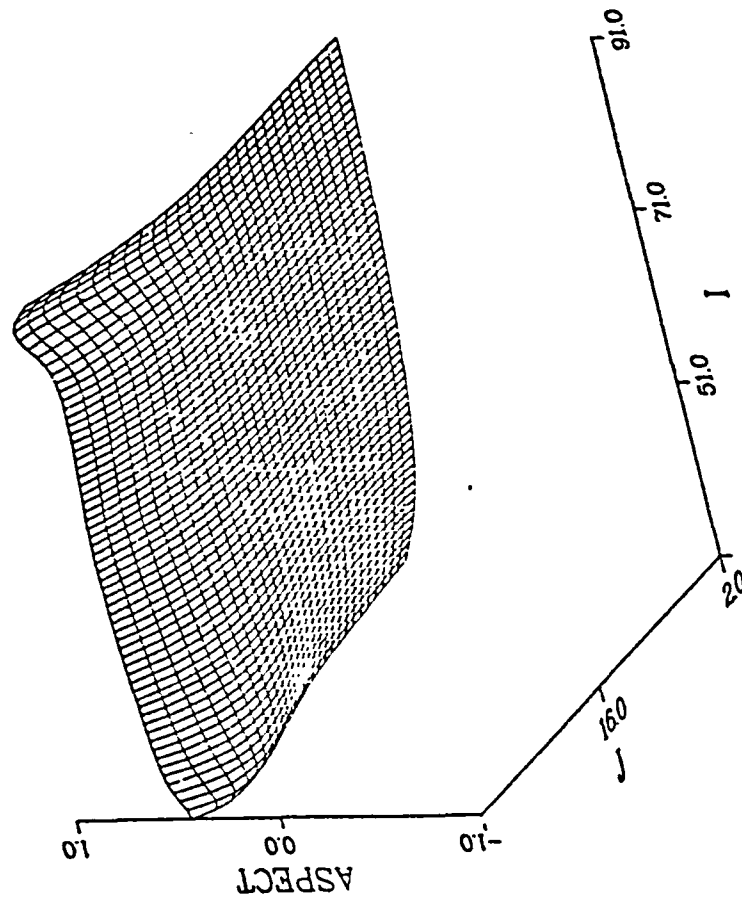
Figure 10. Carpet plot of cell aspect ratio normalized by 1.00.
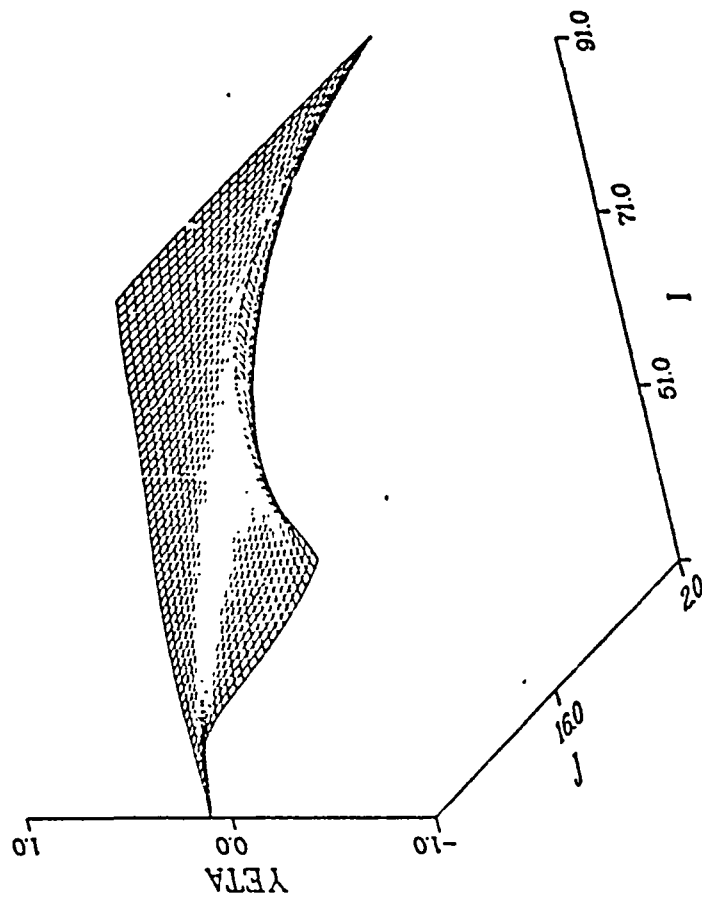
Figure 11. Carpet plot of y_η normalized by 0.3993.
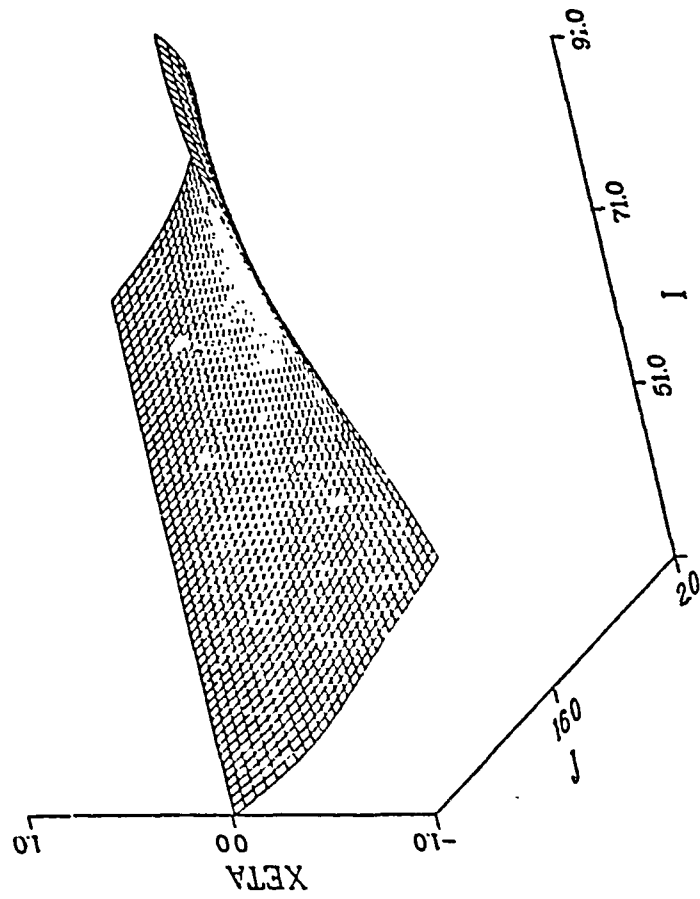
Figure 12. Carpet plot of x_η normalized by 0.6653.
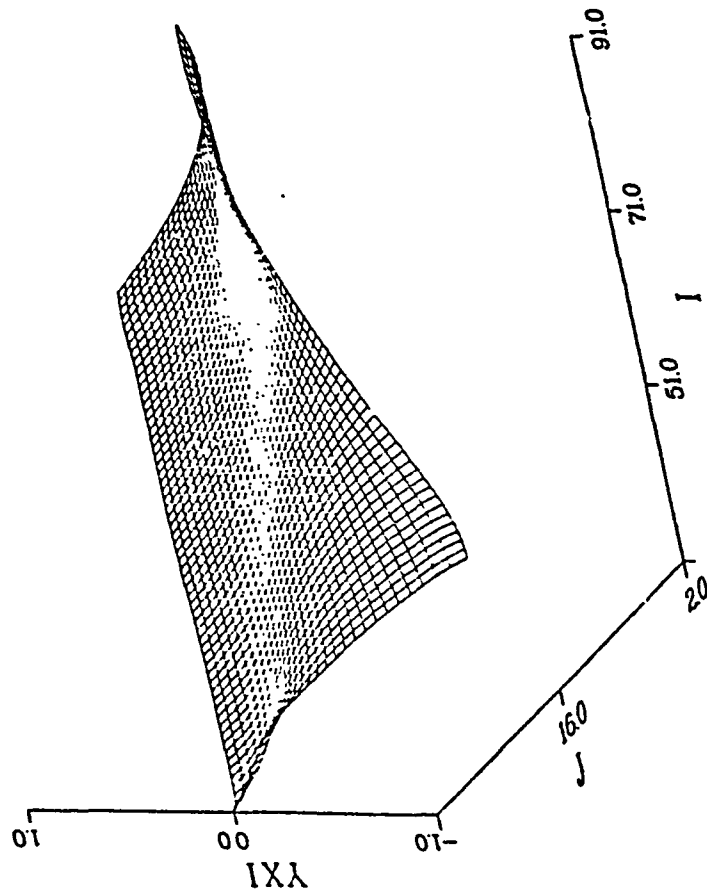
Figure 13. Carpet plot of y_ξ normalized by 0.1773.
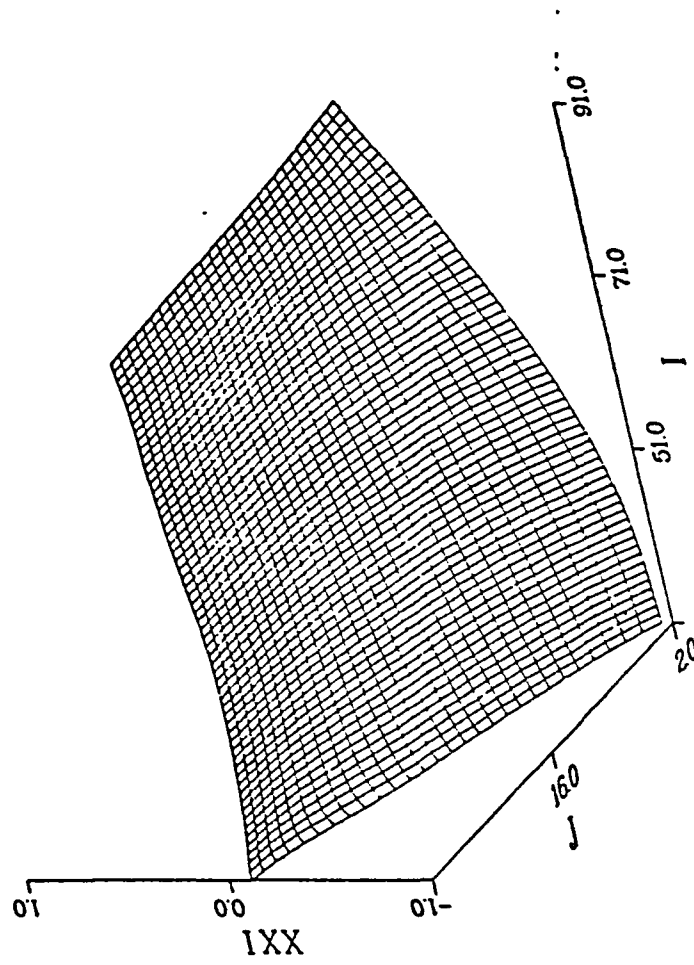
Figure 14.   Carpet plot of x_ξ normalized by 0.1773.

56
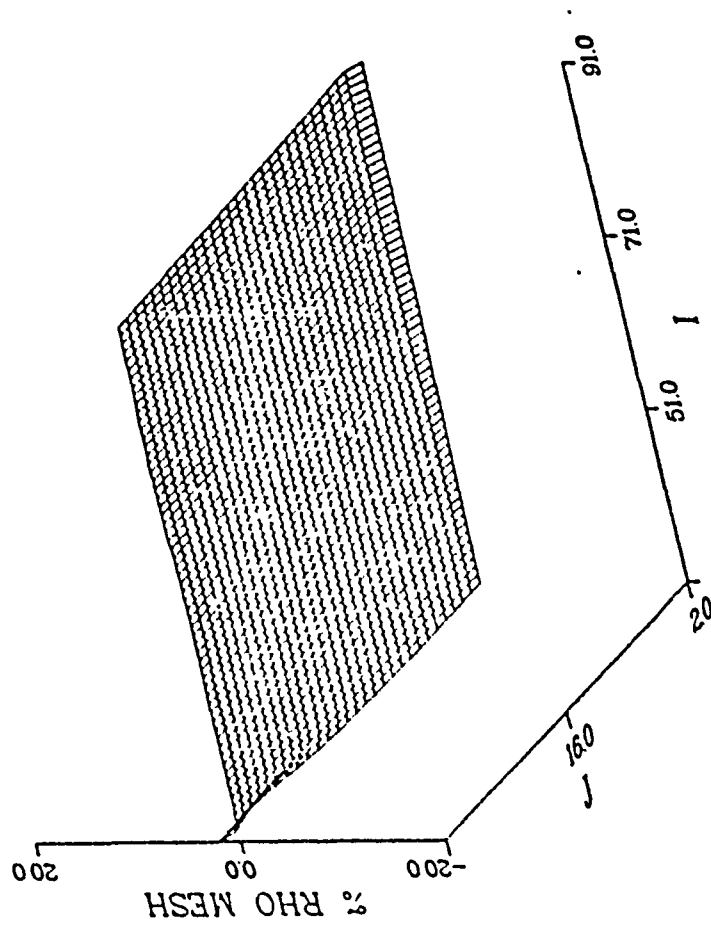
Figure 15. Mesh induced truncation error of density solution shown in figures 2 and 3.
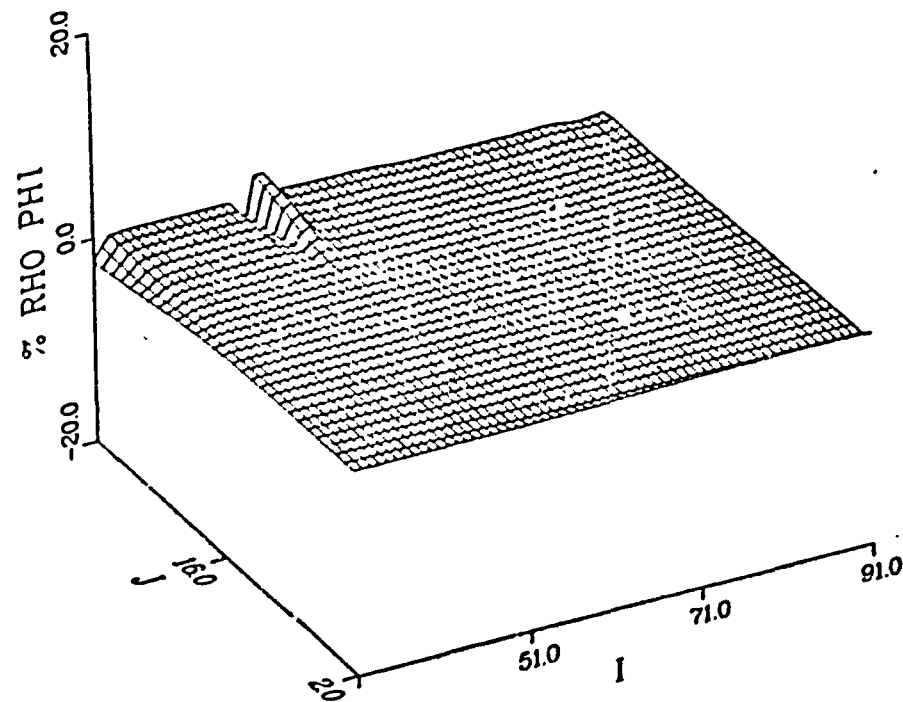
Figure 16.   Solution induced truncation error of density
solution in Figures 2 and 3.
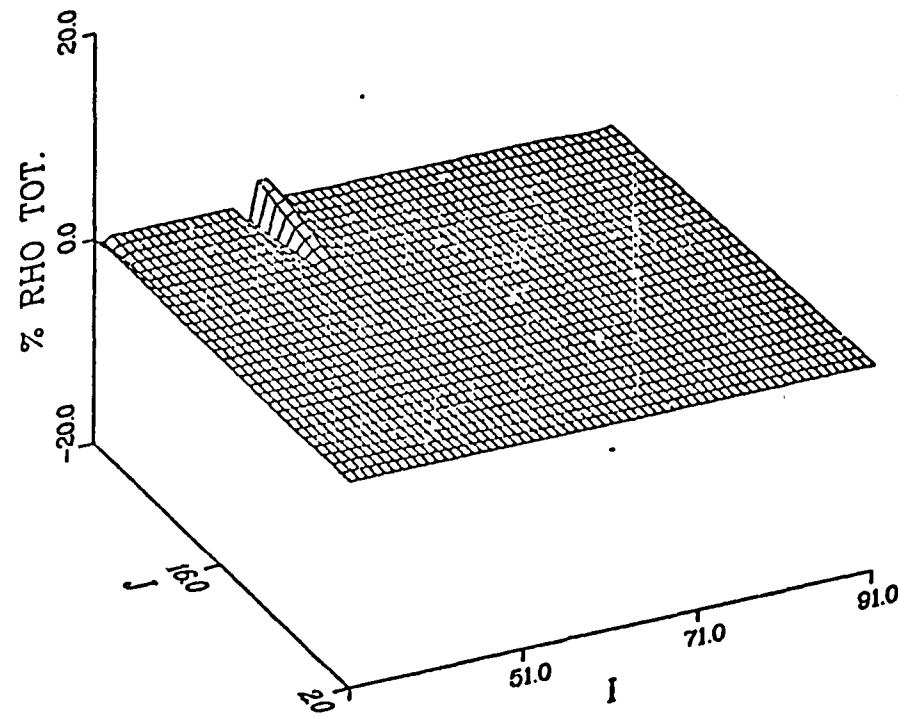
Figure. 17.   Total truncation error of density solution shown in figures 2 and 3.

End of Document